JOURNAL OF QUATERNARY SCIENCE (2022) 1–20 ISSN 0267-8179. DOI: 10.1002/jqs.3412

JQS Journal of Quaternary Science QRA Quaternary Research Association

The development and impact of an ice-contact proglacial lake during the Last Glacial Termination, Palaeolake Riada, central Ireland

CATHERINE DELANEY*
Department of Natural Sciences, Manchester Metropolitan University, Manchester, UK

Received 30 July 2021; Revised 13 January 2022; Accepted 4 February 2022

ABSTRACT: The retreat of the last Irish Ice Sheet across the Irish midlands resulted in the formation of an ice-contact lake, Palaeolake Riada, along its eastern margin during recession. However, the full extent and characteristics of the lake and its impact on ice dynamics are unknown, as glacigenic landforms and deposits relating to the lake have not been mapped in sufficient detail to allow reconstruction of ice-marginal behaviour. This paper presents new mapping of subglacial, ice-marginal and glaciolacustrine landforms and deposits in the Irish midlands. Glacial landforms and landform associations across this wide area have been identified using aerial photographs and high-resolution digital elevation models derived from LiDAR and radar data. Reconstructions of successive ice-margin retreat positions are combined with glacio-isostatically adjusted digital elevation models to identify the probable position of lake outflows and reconstruct the development of the proglacial Palaeolake Riada through time. These reconstructions indicate that at its largest, Palaeolake Riada had an ice-contact margin of 113 km, and covered an area of over 2300 km^2. Initially, ice recession was concentrated around meltwater discharge outlets, but these became less important as the lake expanded and thermo-mechanical erosion occurred along the entire subaqueous margin.

KEYWORDS: glaciolacustrine; Irish Ice Sheet; Last Glacial Termination; Midlandian; Palaeolake Riada; proglacial lake

Introduction

The recent, climate-driven, retreat of ice sheets and glaciers has led to an expansion in the number and size of proglacial lakes, dammed between the ice margin and enclosing topography (e.g. bedrock or glacial deposits; e.g. Schomacker, 2010; Carrivick and Quincey, 2014; Buckel *et al.*, 2018; Shugar *et al.*, 2020). Both modern and Quaternary examples indicate that these lakes have a major impact on glacier dynamics during ice-sheet recession, partly decoupling glacier behaviour from climate forcing. The effects on ice masses include changes in ice flow direction (Carrivick and Tweed, 2013; Storrar *et al.*, 2017; Dell *et al.*, 2019) and velocity (Stokes and Clark, 2003; Dell *et al.*, 2019; Ponce *et al.*, 2019; Baurley *et al.*, 2020; Sutherland *et al.*, 2020) and the acceleration of ice recession in comparison with adjacent land-terminating glaciers, partly decoupling ice dynamics from climate (Benn *et al.*, 2007; Schomacker, 2010; Sutherland *et al.*, 2020; Kellerer-Pirklbauer *et al.*, 2021). The presence of a waterbody at the ice margin also affects the meltwater and sediment discharge, causing a rapid deceleration of flow and the formation of sedimentary landforms (Ashley, 1995; Teller, 2005). The deposition of fine-grained, distal glaciolacustrine sediment can also influence ice dynamics, as this sediment offers little frictional resistance and may help promote or enhance an ice-marginal readvance (Smith, 1990; Bateman *et al.*, 2018). Identification of Quaternary proglacial lakes is therefore an important element in palaeoglaciological reconstruction of former ice-sheet and glacier extents and behaviour.

Reconstructions of the last British–Irish Ice Sheet (*c.* 30–14.5 ka BP) play an important role in the development and improvement of numerical ice-sheet models used to predict future ice-sheet responses to climate change (e.g. Hubbard *et al.*, 2009; Clark *et al.*, 2012; Gandy *et al.* 2019). A well-preserved glacial 'footprint' indicates that the British–Irish Ice Sheet was highly dynamic, reflecting its relatively small size and southerly position on the eastern Atlantic margin. For the British Ice Sheet, extensive proglacial lakes are known to have formed at its onshore-terminating margins (e.g. Murton and Murton, 2012; Emery *et al.*, 2019), and recent reconstructions of ice-sheet configuration through time have demonstrated the impact of these lakes on ice dynamics (e.g. Bateman *et al.*, 2018; Chiverrell *et al.*, 2020). Proglacial ice-contact lakes have also been identified along the margins of the Irish Ice Sheet (IIS) during its onshore recession (Charlesworth, 1928, 1939; Farrington, 1957, Dardis, 1986; Van der Meer and Warren, 1997; Pellicer *et al.*, 2012; McCarron, 2013; Philcox, 2019). However, with the exception of Glacial Lake Blessington, very little information is available about the development of these lakes, the associated deposits, or their impact on ice dynamics.

The aim of this paper is to reconstruct the development of a large proglacial lake, Palaeolake Riada (Pellicer *et al.*, 2012), which formed along the southeastern margin of the IIS during the Last Glacial Termination (after 22 ka BP), in order to establish the changing lake extent and its impact on the ice-margin geometry and ice-marginal ice dynamics of the Late Midlandian IIS during the later stages of its retreat. This paper examines morpho-sedimentary evidence for the lake in the catchments of the River Shannon and its tributaries, the Brosna, Little Brosna, Inny and Suck rivers, in the Irish midlands (Fig. 1). The changing extent of the lake is reconstructed by identifying landforms with flat surfaces

*Correspondence: C. Delaney, as above.
Email: c.delaney@mmu.ac.uk

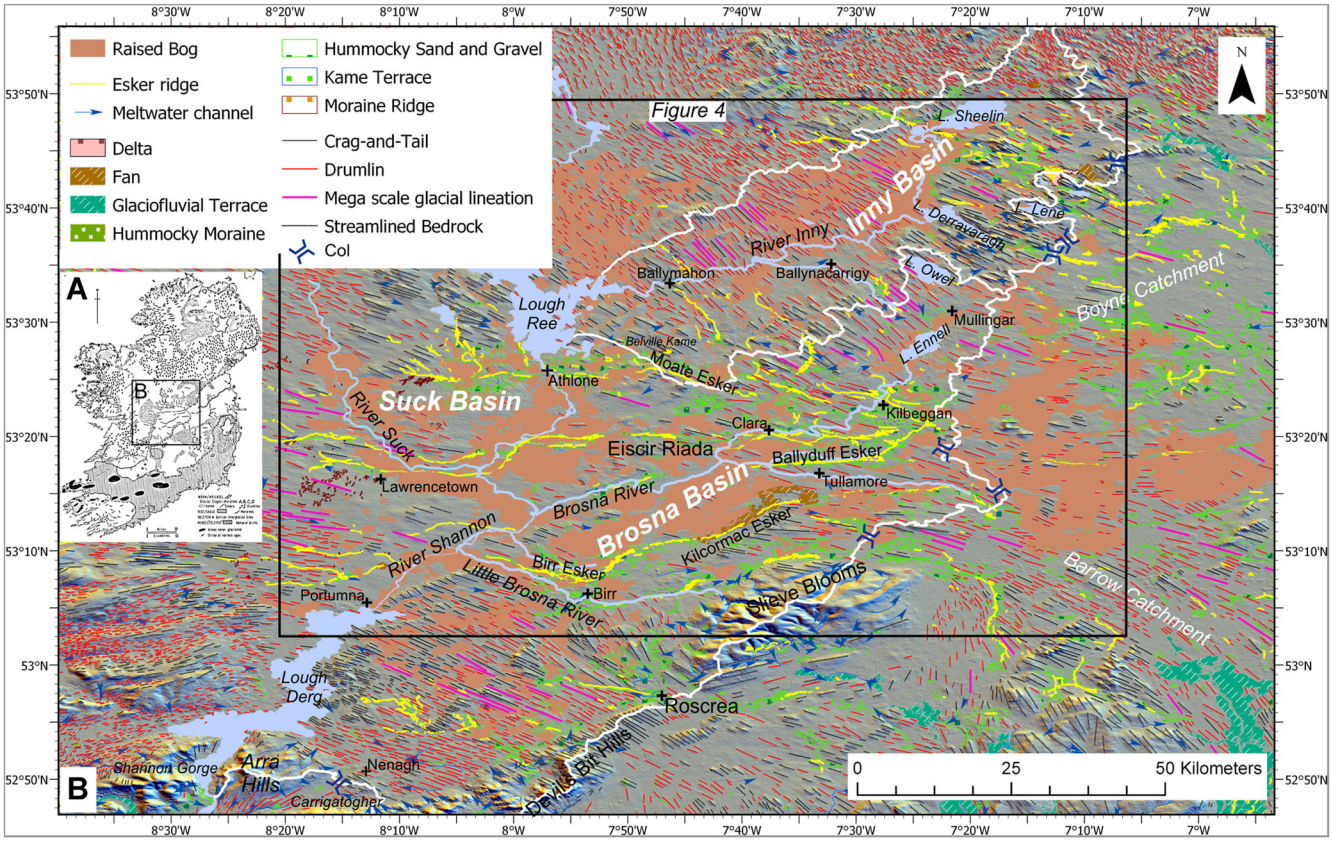

Figure 1. A. Map of Ireland showing main glacial features and the area shown in B (after Synge, 1979; redrawn by P. Coxon). B. Map of area discussed in this paper showing main topographical features, glacial lineations, glaciofluvial features, moraines and meltwater channels as mapped by the Geological Survey of Ireland (2017), and the location of places and features mentioned in the text, showing modern rivers and lakes, position and names of eskers and extent of peat and position of the watersheds and places named in the text. [Color figure can be viewed at wileyonlinelibrary.com]

controlled by water level, modelling of successive ice-margin and lake outflow positions in relation to these water levels and applying a glacio-isostatic adjustment (GIA) model to assess the impact of isostatic depression on lake bathymetry, area, volume and water-surface height. Finally, the study considers the impact of the lake on ice dynamics, using reconstructed ice-flow dynamics inferred from glacial landform patterns and associations in the area. Reconstructing such proglacial lakes is important to correctly model ice-margin retreat and ice-sheet dynamics and to elucidate controls on deglaciation for terrestrial ice sheets.

Previous work

Warren (1991) first proposed the existence of an ice-dammed proglacial lake in the Irish midlands, beginning in the catchment of the River Brosna, a tributary of the River Shannon (Fig. 1). He suggested that the lake had been ice-dammed on all margins, trapped between two ice domes extending southeastward and northwestward. Delaney (2002a) showed that this ice-sheet geometry was unnecessary and that a proglacial ice-dammed lake formed in the Brosna, Little Brosna, Shannon and Suck River catchments, dammed between a westward-retreating ice margin, the Slieve Bloom massif to the south, and the watershed between the Shannon–Boyne and Shannon–Barrow catchments to the east. The lowest point on the Shannon–Boyne watershed, at 87 MOD (metres above ordnance datum), was the same as the delta kame surface at Belville, east of Lough Ree (Fig. 1; Delaney, 2002a).

Van der Meer and Warren (1997) suggested that such a lake could have expanded as the ice retreated and separated into two domes, damming a water body that could have extended northeast to the Lough Neagh basin and southwest to Lough Derg, depending on the ice-retreat pattern (Fig. 2a). Subsequent work by Pellicer *et al.* (2012) utilised the height and location of ice-contact deltas to recreate five lake stages as the postulated lake expanded between two ice lobes retreating west and northwest (Figs. 2b, c). Pellicer and Warren (2005) gave the palaeolake the name Riada, after the Eiscir (esker) Riada, which lies within the lake basin (Fig. 1).

Further evidence for a former glacial lake includes the presence of glaciofluvial deltas and subaqueous outwash fans at the downstream end of conduit fills (eskers; Gallagher *et al.*, 1996; Delaney 2001, 2002a, b; Pellicer *et al.*, 2012, Delaney, 2019) and deposits of glaciolacustrine inorganic, laminated silt and clay that underlie the extensive peat and Holocene lake sequences on either side of the Shannon River and within the Brosna catchment (Van der Meer and Warren, 1997; Long and O'Riordan, 2001; Delaney, 2007; Long, 2019).

However, a significant issue in constraining the lake extents over time is the absence of evidence for ice-marginal positions in the central Irish midlands (Fig. 3; Greenwood and Clark, 2009b). The existence of evidence indicating the presence of a regionally important ice margin contiguous with moraines on the Irish Sea coastline was first proposed in the early 20th century (Charlesworth, 1928; Synge, 1952). Moraines around Dundalk Bay are thought to have formed during the Killard Point Stadial, during a readvance that reached its maximum at *c.* 17 ka cal. BP (McCabe, 2007; Chiverrell *et al.*, 2013). On the west coast, moraines south of the

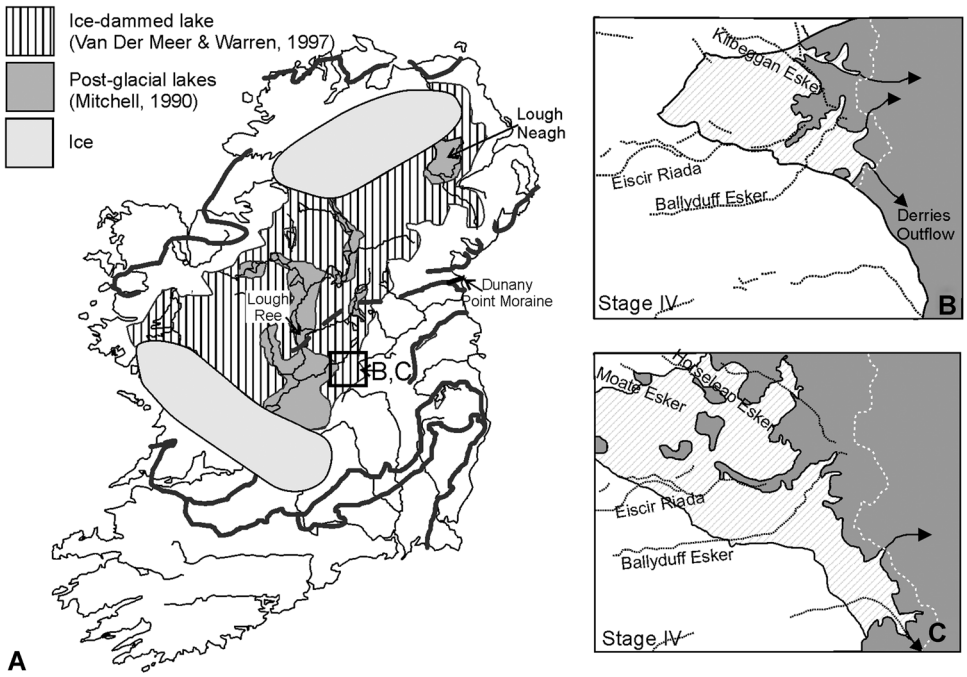

Figure 2. A. Potential extent of ice-dammed and early post-glacial glacio-isostatically controlled lakes in the Irish midlands, as proposed by Van der Meer and Warren (1997) and Mitchell (1990). B and C. Successive models for the earliest stages of Palaeolake Riada, redrawn from Pellicer *et al.*, (2012)

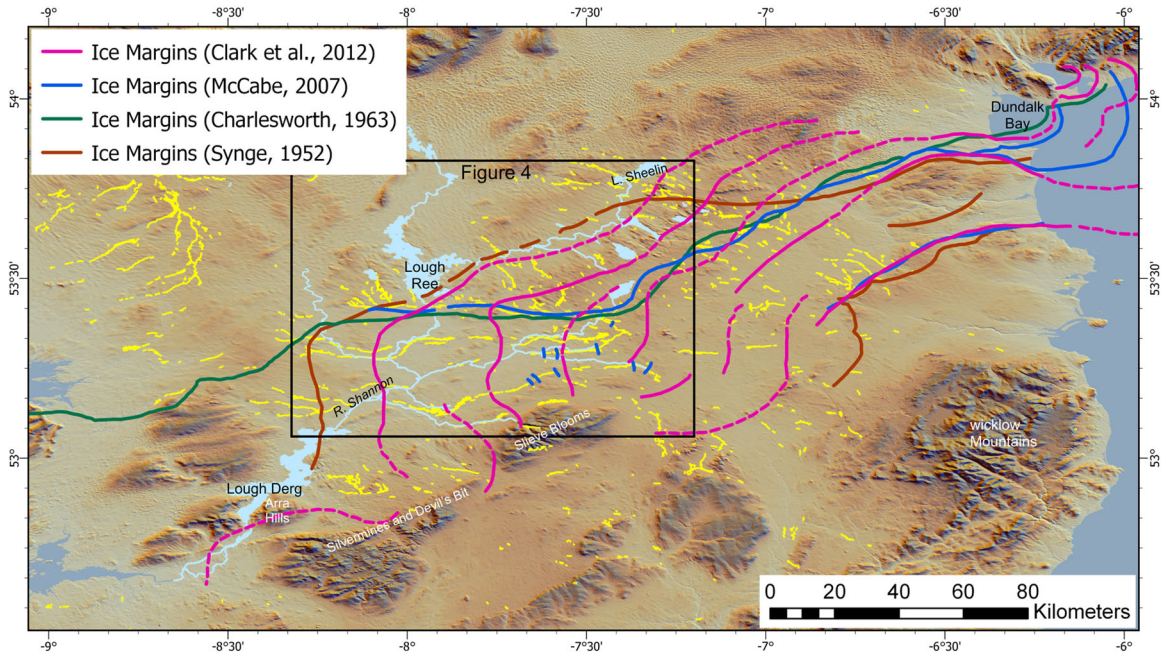

Figure 3. Published models for ice-margin positions across the Irish midlands. The box shows the position of the study area shown in Fig. 1B. [Color figure can be viewed at wileyonlinelibrary.com]

Shannon estuary are correlated with the Dundalk Bay moraines (Synge, 1952; Clark *et al.*, 2012). However, significantly different models exist for the position of the ice margin within the central midlands (Fig. 3; Synge, 1952; Meehan, 2004; McCabe, 2007; Clark *et al.*, 2012). Variations in reconstructed ice-sheet geometry result from the absence of large moraines and the dependence on glaciofluvial ice-marginal landforms for reconstructing ice-margin positions (e.g. Warren and Ashley, 1994; Delaney, 2002a; Pellicer *et al.*, 2012). In addition, no points of geochronological control are currently available for deglaciation of the Irish midlands (Clark *et al.*, 2021).

The study area

Regional geology and topography

The central Irish midlands consists of a low-lying plain (~40–80 MOD), drained by the River Shannon and its tributaries, with some hills up to ~200 MOD (Fig. 1). In this study, the area is divided into three drainage basins, named after the largest river in each: 1) the Brosna basin, covering the Brosna and Little Brosna catchments and the area east of the River Shannon between Lough Ree and Lough Derg; 2) the Suck basin, covering the Suck catchment and the area west of the River Shannon between Lough Ree and Lough Derg; and

3) the Inny basin, covering the Inny catchment and the area draining directly into Lough Ree along its eastern margin (Fig. 1).

The dominant bedrock is Carboniferous limestone, with inliers of Palaeozoic sandstone and siltstone underlying areas of higher ground that extend generally northeast southwest across the area (Sevastopulo and Wyse-Jackson, 2009). To the south, the Slieve Bloom massif (480–514 MOD) marks the southern boundary of the Brosna and Little Brosna catchments.

Regional glacial landform and sediment distributions

Larger glacial landforms and deposits dating from the last glaciation (Late Midlandian, *c.* 30–14.5 ka BP) have been mapped previously (e.g. Greenwood and Clark, 2008, 2009a, b; GSI, 2017). Most of the area is covered by glacigenic sediments (diamictons, sand and gravel) and Holocene wetland sediments, including raised bog, fen, lacustrine and alluvial sediments in the lower areas and around rivers (Fig. 1; GSI, 2017). Bedrock is occasionally exposed on higher ground. In general, till composition reflects bedrock geology immediately up-ice, with limestone tills dominating. In the Inny basin, sandstone tills occur in the northern part of the basin, and chert-rich tills in the southwest. In the north and west the landscape is dominated by subglacial lineations, including drumlins, mega-scale glacial lineations (MSGLs), crag-and-tails and streamlined bedrock (Fig. 1; GSI, 2017). Lineation alignment is dominantly southeast to south-southeastward, with eastward-oriented MSGLs at the eastern end of the Brosna basin (Delaney *et al.*, 2018). Several overlapping flowsets have been identified, indicating shifts in ice-flow dynamics through time (Greenwood and Clark, 2009a, b; Delaney *et al.*, 2018). Crevasse-squeeze ridges (CSRs) also occur in the southern part of the area, formed after episodes of accelerated ice flow.

The dominant landform in the south and east are eskers and associated glaciofluvial and glaciolacustrine deposits. There are two esker systems: the Midlands system, extending eastward across the Suck and Brosna river basins; and the Lough Ree system, extending south-southeastward to south-eastward from the Suck and Inny basins to the northern margin of the Brosna basin (Fig. 1; Sollas, 1896; Flint, 1930; Delaney, 2002a; McCabe, 2007). Eskers are generally aligned parallel to adjacent lineations and comprise discontinuous ridges, or long beads, consisting of conduit fills leading downstream to fan-shaped or flat-topped areas underlain by well-sorted gravel, sand and fines, discussed further below (Fig. 4; Farrington and Synge, 1970; Warren and Ashley, 1994; Delaney, 2001, 2002a, b; Pellicer *et al.*, 2012). Beads are between 1 and 5 km in length.

Moraines are rare but do occur at the eastern end of the Brosna basin, where they converge on the Eiscir Riada, with ridges to the south aligned north–south and those to the north of the esker aligned northeast–southwest (Pellicer *et al.*, 2012; Delaney, 2019).

Methods

Geomorphology and sedimentology

In order to reconstruct the evolution of Palaeolake Riada, new geomorphological and sedimentary evidence was collected. Geomorphological mapping was undertaken using a combination of aerial photographs (from Google Earth Pro Historical Imagery and the Ordnance Survey of Ireland online viewer), high-resolution digital elevation models (DEMs) constructed

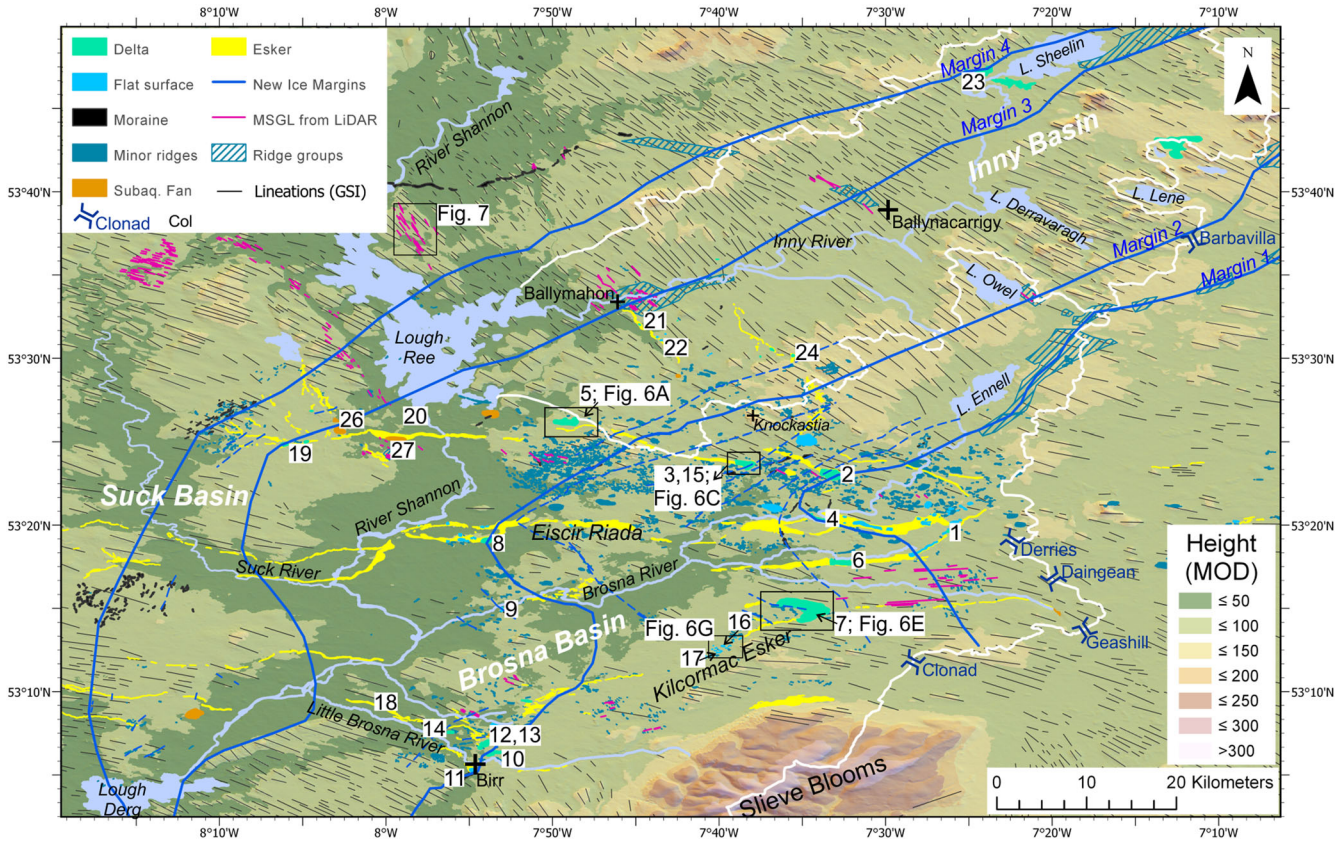

Figure 4. Map of area showing glacial features mapped as part of this study, plus glacial lineations mapped by the Geological Survey of Ireland (2017), locations of features discussed in the text, and ice-margin positions inferred from new mapping of glacigenic features. [Color figure can be viewed at wileyonlinelibrary.com]

from airborne LiDAR (resolution 0.5–1 m; available from the Geological Survey of Ireland online viewer), and radiometric terrain corrected (RTC) high-resolution DEMs (12.5 m resolution; ASF DAAC, 2015). LiDAR DEMs were preprocessed to remove trees and buildings, still present in the RTC DEMs. All DEMs were processed to produce multidirectional hill-shaded views using the Relief Visualisation Toolbox (Kokalj *et al.*, 2011; Zakšek *et al.*, 2011). Particular attention was given to mapping glacial lineations, ice-flow transverse ridges and flat-topped landforms that indicate that water level controlled their formation, either by wave erosion or by acting as an upper limit for deposition (Table 1). Landform height and profiles were extracted from DEMs and elevations are given in relation to the ordnance datum based on mean sea level at Malin Head. The location and nature of landforms was confirmed by fieldwork.

Exposures in glaciolacustrine landforms were located from aerial photos and field surveys and used to identify sedimentary lithofacies and deposit architecture. Sediments were described using standard approaches and classified using lithofacies codes (detailed in supporting information Table S1; Evans and Benn, 2004). Sediments were initially grouped into lithofacies associations (LFAs) to aid interpretation and these are presented in the supporting information, Table S2.These were then further grouped into morpho-sedimentary associations (MSAs) on the basis of association between LFAs and specific landform or terrain types.

Reconstruction of lake extents

Reconstructions of ice-dammed lakes rely on the identification of two key features: 1) successive ice-margin positions during ice recession; and 2) likely outflow channels operating for each ice-margin position (Utting and Atkinson, 2019). These are checked against the location of glaciolacustrine landforms, and are used to establish the position of ice dams and exclude lower elevation areas blocked by ice from acting as outflows. This approach has limitations as water is likely to escape from a proglacial lake by moving over or through a blocking ice body, a drainage pathway that will become more likely as the ice thins vertically, so lake extents and heights modelled should be regarded as maximum estimates.

In order to establish lake extent, ice-marginal positions were reconstructed from a combination of ice-flow transverse ridges and ice-contact glaciofluvial landforms in the study area. Outside the study area, the positions of ice margins are based on orientations from Clark *et al.* (2012; Fig. 3), together with identification of ice-flow transverse ridges on LiDAR DEMs (Fig. 4).

To accurately identify lake outflows and model lake extent, adjustment to the landscape elevation surface on which lake extent is modelled is required, in order to subtract the differential impact of post-glacial glacio-isostatic rebound across the area, particularly as Palaeolake Riada extended parallel to the gradient of glacio-isostatic tilt (e.g. Bradley *et al.*, 2011; Edwards and Craven, 2017; Shennan *et al.*, 2018). In order to apply a GIA model, it was necessary to establish an age for each identified ice margin. Due to the absence of a geochronology in the study area, the reconstructed ice margins were linked to securely dated glacial features at the coastline, dated between 17 and 16 ka BP, using a combination of published reconstructions of the ice margins and newly identified ice-marginal features.

The BRADLEY2017 GIA model was applied to a 25 m resolution DEM (the EU-DEM, selected because it provided full coverage for the area) in order to adjust surface elevation and constrain outflow elevations and lake extent (Fig. 5). This GIA model is constructed in 500-year time slices, with a 35 km^2 resolution (Shennan *et al.*, 2018).

Outflow positions were identified using model outputs. The positions of outflows were located by identifying the lowest elevation cols crossing the watershed in front of each

Table 1. Flat-topped features in the study area.

Number (Fig. 4)	Name	Height MOD (Malin)	Height related to	Type of feature
Brosna catchment				
1	Bracklin Little	90 m	Surface	Shoal delta
2	Horseleap	88–90 m	Topset-foreset	Gilbert delta
3	Moate	83 m, 76 m	Surface	Gilbert delta
4	Clavin's Hill	87 m	Surface (topsets absent)	Gilbert delta
5	Belville	85 m	Topset-foreset	Gilbert delta
6	Ballyduff	77 m	Surface	Wave-dominated delta
7	Blackwood	75–78 m	Topset-foreset	Wave-dominated delta
8	Esker Hill	77 m	Surface	Wave-dominated delta
9	Ballingowan	75 m	Surface	Gilbert delta
10	Lisheen (Birr)	71–73 m	Surface	Gilbert delta
11	Drumbane (Birr)	64–68 m	Surface	No topsets exposed
12	Knockydowny (Kennedy's Cross)	68 m	Surface	Gilbert delta
13	Tullynisk (Birr)	71 m	Surface	No topsets exposed
14	Glaster (nr Birr)	61 m	Surface	No topsets exposed
15	Moate	65 m	Terrace	Shoreline
16	Killooly N (Kilcormac esker)	69, 73, 76 m	Terrace	Shoreline
17	Derrydolney (Kilcormac esker)	69,70, 72 m	Terrace	Shoreline
18	Birr Esker	55, 60 m	Terrace	Shoreline
Suck catchment				
19	Eskerbeg	69–70 m	Surface	No topsets exposed
20	Barrybeg	39 m	Surface	Shoreline
Inny catchment				
21	Keel, Ballymahon Esker	63–64 m	Surface	Gilbert delta
22	Calliaghstown (Ballymahon esker)	64–65 m	Surface	Shoreline
23	Lough Kinale	73–74 m	Surface	No topsets exposed
24	Washford	107 m	Surface	Shoal delta

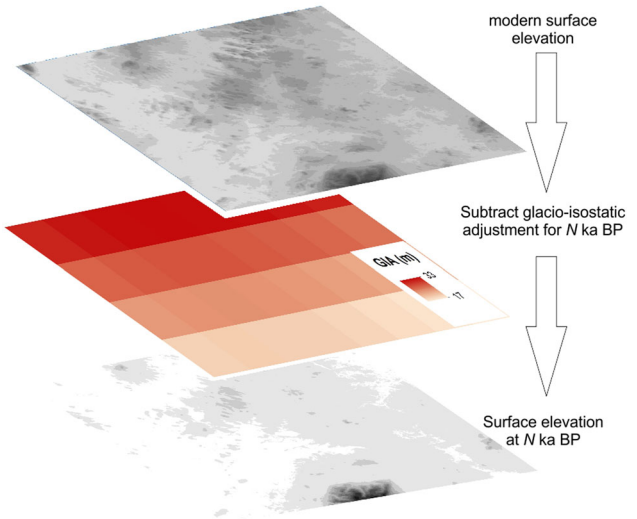

Figure 5. Glacio-isostatic adjustment of a digital elevation model for a specific time slice. [Color figure can be viewed at wileyonlinelibrary.com]

reconstructed ice margin. Col heights were then compared with the nearest flat-topped landforms, to establish whether the features were formed contemporaneously. Finally, lake extent was reconstructed for each stage by modelling a horizontal water surface using the outflow col elevations to constrain water levels. Lake area and volume were calculated using the surface volume function in ArcGIS.

Results

Geomorphology

Glaciofluvial/glaciolacustrine flat-topped landforms

Three types of glaciofluvial/glaciolacustrine landforms were observed:

(i) *Type 1 kames*: these are high (7–40 m), flat-topped, steep-sided landforms, commonly located on the downstream end of esker ridges composed of conduit and channel sediments (Fig. 4). Ice-proximal slopes are steep (15–25°; Fig. 6E, F); distal slopes are gentler and often stepped (5–20°; Fig. 6E, F). The features extend both parallel and transverse to ice flow direction; flow-parallel features commonly have steep side slopes (Fig. 6A–D); flow-transverse features often have a prominent ridge along the ice-proximal side (Fig. 6E, F). Landform surfaces lie between 90 and 61 MOD. The highest are along the northern and far eastern margin of the Brosna basin (surfaces between 90 and 83 MOD; features 1–5 in Table 1; Fig. 4) and the southern and far eastern margin of the Inny basin (107–140 MOD; 24 in Table 1; Fig. 4). Surfaces become progressively lower westward, and are below 70 MOD in the Suck basin. Surface height is most variable around Birr (82–64 MOD; 10–14 in Table 1; Fig. 4).

(ii) *Type 2 kames*: these are small (area <0.1 km^2, usually <0.05 km^2), low (<10 m high) flat-topped mounds with no clear orientation. They occur in clusters of several distinct mounds, sometimes linked by short necks (Fig. 6G, H). One cluster along the northern margin of the Kilcormac esker forms a band up to 2 km wide and 9 km long parallel to the esker (Figs. 4, 6G, H; features 16, 17 in Table 1). Landform elevations in this area lie between 65 and 70 MOD, similar to elevations of terraces cut in the adjacent esker. A second cluster at the eastern end of the Brosna basin forms a 4 km by 2 km zone extending roughly north–south, east of the eastern end of the Eiscir Riada (Fig. 4). The landform surfaces are at 106–75 MOD.

(iii) *Shoreline terraces*: these occur along the side of eskers. They are well-developed in the southern Brosna basin, particularly on the Kilcormac and Birr eskers, but are also present along the northern margin on the Moate esker, where there is a terrace at *c.* 65 MOD, and further small terraces occur on the southwestern margin of the esker at about 63 MOD (Figs. 4, 6C, D; feature 15 in Table 1). On the Kilcormac esker, two terraces occur at *c.* 75 MOD and at 65 MOD, with an inflexion point at 70–71 MOD (Fig. 6G, H; features 16–17 in Table 1).

Subglacial lineations

Drumlins have been mapped previously by the GSI (2017). New MSGLs identified on LiDAR DEMs are shown in Fig. 4; these are <2 m (often <1 m) high and between 800 and 4000 m long, but are often fragmented (Fig. 4; Delaney *et al.*, 2018; Delaney *et al.*, in prep.). In the southern Brosna basin, these are aligned southeastward (Fig. 4). Along the northern margin of the Brosna basin, MSGL alignment is east-southeastward, parallel to the southern end of the Lough Ree esker system. Around the margins of Lough Ree, MSGLs are aligned north-northwest to south-southeast, parallel to the long axis of the lake, and at a more southerly orientation than the underlying drumlins (Figs. 4, 7).

Ice-flow transverse ridges

Groups of small (<5 m high, <200 m long), ice-flow transverse ridges are common throughout the study area, in areas previously mapped as hummocky topography associated with stagnant ice (Charlesworth, 1928; Figs. 4, 6A, B; Delaney *et al.*, 2018). Within the Brosna basin, these ridges converge on the Eiscir Riada (Fig. 4). North of the esker, parallel bands of small ridges aligned east-northeast to west-southwest were traced to the Irish Sea coastline around Dundalk Bay (see below), and west of the Shannon on either side of Lough Ree (Fig. 4). In the eastern Brosna basin, ridges are aligned west-northwest to east-southeast on the southern side the Eiscir Riada. This orientation changes westward, to near north–south immediately south of Clara (Figs. 1, 4) and varies between north–south and northwest–southeast toward the Shannon. A large group of north–south-oriented ridges are present in the Suck basin south of the Eiscir Riada (Fig. 4).

Along the southern margin of the Brosna basin, around the Kilcormac esker, ice-flow transverse ridges also shift orientation, from north–south in the east, to west-northwest to east-southeast and northwest – southeast further west, at right angles to MSGLs (Fig. 4).

Morpho-sedimentary associations

Ten LFAs were identified (Table S2) and these have been grouped into five MSAs, based on their association with specific geomorphological features.

MSA 1 Gilbert-type deltas

MSA 1a classic Gilbert-type deltas: larger Type 1 kames are underlain by sediments exhibiting distinct topset-foreset-bottomset clinoforms (LFAS 1, 3, 4; Table S2; Fig. 8A) characteristic of classic Gilbert deltas (Gilbert, 1885). Topsets usually have an erosional contact with the underlying foresets.

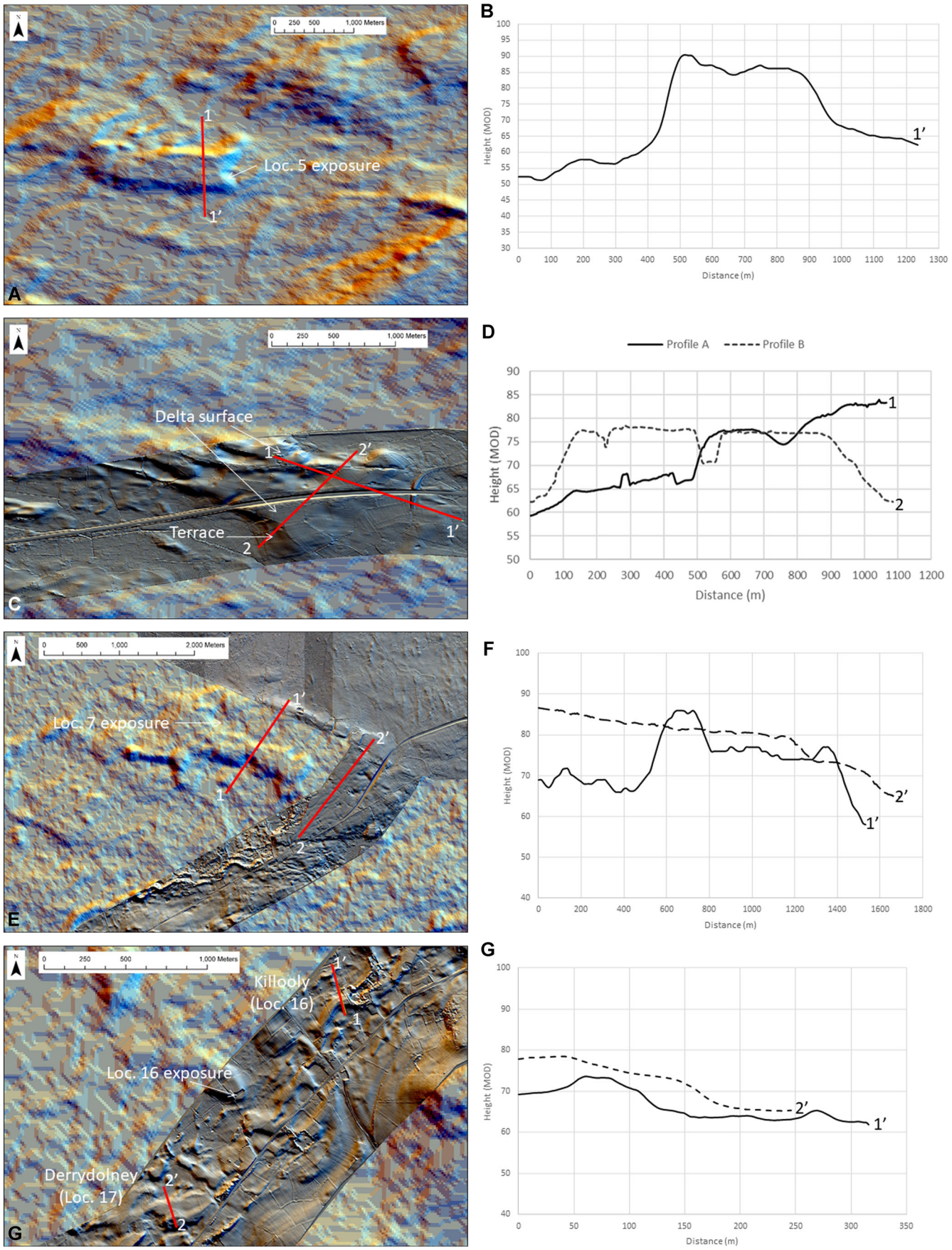

Figure 6. Radar and LiDAR hillshaded DEMs and profiles (12.5 m and 1 m resolution) of landforms in the study area. Locations are shown on Fig. 5. A. Location 5: Gilbert-type delta, northern Brosna basin (12.5 m resolution). B. Profile across the Location 5 delta. C. Combined 12.5 and 1 m resolution DEM showing the Gilbert-type delta at Location 3, the terminus of the Moate esker, northern Brosna basin. D. Profiles across the Location 3 delta showing the stepped surface. E. Combined 12.5 m and 1 m resolution DEM of Location 7 delta and fan complex, southeast Brosna basin. F. Profiles across the Location 7 delta and fan. G. 12.5 m and 1 m resolution DEM of terraces developed along the side of the Kilcormac esker, southern Brosna Basin. Position of exposure at Location 16 is indicated. H. Profiles across the Kilcormac esker and adjacent landforms. Radar DEM ASF DAAC 2015; Includes Material © JAXA/METI 2007. [Color figure can be viewed at wileyonlinelibrary.com]

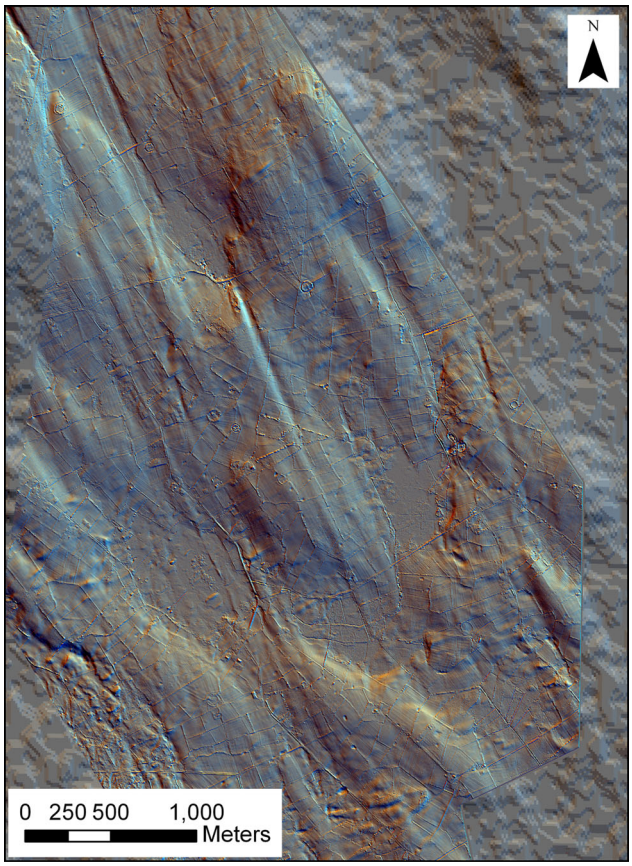

Figure 7. 1 m resolution hillshaded LiDAR DEM (combined with 12.5 m Radar DEM) showing MSGLs overlying drumlins east of Lough Ree. Small ice-flow transverse ridges are imposed on both types of feature. Location shown on Fig. 5. Radar DEM from ASF DAAC 2015; Includes Material © JAXA/METI 2007. [Color figure can be viewed at wileyonlinelibrary.com]

The largest deltas observed have laterally variable foreset sequences. Debris flow-dominated foresets were observed in all delta exposures, indicating episodic deposition from high-density mass flows and falls (Fig. 8A, D; LFA 3; Table S2; Nemec, 1990; Gobo *et al.*, 2014, 2015; Winsemann *et al.*, 2018). Foresets are largest in the lowest parts of the Brosna basin, where they reach heights of up to 20 m (features 5, 8 in Table 1). In larger deltas these are succeeded by density current-dominated foresets (LFA 4; Table S2; Fig. 8E, F). These are shorter (heights <12 m) with lower dip angles, with sedimentary structures indicative of super-critical flow, including cyclic steps, antidunes and scours associated with hydraulic jumps, separated by lower-flow regime bedforms and drape lamination. These foresets grade laterally into toesets (Fig. 8E; LFA 6; Table S2) and bottomsets (Fig. 10E; LFA 7; Table S2) indicating further deceleration.

MSA1b wave-dominated Gilbert-type deltas

Wave-dominated deltas are similar to classic Gilbert-type deltas, but with topsets characterised by beach face and shore face facies (LFA 2; Table S2; Fig. 8C). At Location 6 (Table 1; Fig. 4) beach face sediments consisting of well-sorted, thinly bedded pebble and cobble gravels extend along the top of the delta for over 600 m, exhibiting changes in dip direction and dip angle between 0 and 15°, and overlying distal subaqueous outwash sediments (LFAs 2, 7; Table S2; Fig. 8C). The variable dip direction reflects alongshore variation in beach morphology associated with aggradation of beach berms and the occurrence of overwash (Massari and Parea, 1988, 1990; Blair, 1999; Neal *et al.*, 2002; Pascucci *et al.*, 2009). Other deltas have distal foresets dominated by openwork pebble and gravels that are separated from underlying debris flow and density current-dominated foresets by distinct reactivation surfaces and indicate winnowing and redeposition of topset sediments.

All Gilbert-type deltas occur where the surrounding land surface lies below 70 MOD (Table 1; Fig. 4). In the Brosna basin, the highest delta surfaces occur in the northeast (Locations 2–5; Table 1; Fig. 4). South of the Eiscir Riada, delta surface elevations fall below 80 MOD. Topset–foreset contacts at the eastern end of the basin are at 73–78 MOD (Locations 6, 7; Table 1; Fig. 4; Pellicer *et al.*, 2012), and in the centre of the basin are at 75–77 MOD (Locations 8, 9; Table 1; Fig. 4). Surfaces are lower in the southwest where delta surfaces around Birr are stepped at 71, 68 and 61 MOD (Locations 10–14; Table 1; Fig. 4).

In the Suck basin, one delta was identified, with a surface at 69–70 MOD (Location 19; Table 1; Fig. 4). Other flat-topped features in the area may also be deltaic in origin, or may have wave-cut surfaces. In the Inny basin, three deltas were identified. Two were mapped by the GSI (2017). The Murrens delta (Location 25) in the northeast of the basin is at 115–140 MOD, higher than other deltas. The Kinale delta surface lies at 73–74 MOD (Location 23, Table 1; GSI, 2017). A small delta on the Ballymahon esker at 63–64 MOD (Location 21; Table 1; Fig. 4) is at a similar height to other flat-topped features along the Ballymahon and Moyvore eskers.

MSA 2 shoal deltas

This MSA was identified in two small Type 1 kames at the downstream end of esker ridges–in the Brosna basin at Location 1 (Table 1; Fig. 4) and in the Inny basin at Location 24 (Table 1; Fig. 4). The delta surface at Location 1 is at 90 MOD and is aligned with the Type 2 kame cluster to the north (Fig. 4). The proximal end of the kame is composed of cobble and pebble planar and parallel-bedded gravels with inter-bedded sands forming interdigitating lenses, interpreted as aggrading longitudinal and diagonal bars, with interstratified distal-bar sandy channel fills (LFA 1; Table S2; e.g. Marren, 2005; Fig. 8B). These are succeeded downstream by cross-bedded gravels and then by small-scale, sand-dominated sigmoidal-oblique and sigmoidal clinoforms stacked laterally and vertically (LFA 5; Table S2; Fig. 10A). These interdigitate with bottomset sediments dominated by normally graded coarse to fine sand beds aggrading rapidly upwards into climbing-ripple cross-laminated fine sand and silt (LFA 7; Table S2; Fig. 10A). This sedimentary sequence is typical of mouth bar sequences, formed by aggradation of a shoal delta into shallow water on a low or reverse gradient slope (e.g. Postma, 1990; Winsemann *et al.*, 2009; Eilertsen *et al.*, 2011). The thick bottomsets and evidence for extensive suspension deposition indicates the water was too shallow for stratification and rapid fallout from sediment plumes occurred in front of the delta (Eilertsen *et al.*, 2011).

The delta at Location 24 is at 106 MOD, well above other surfaces in the Inny basin, and consists of a basal unit of horizontally bedded bottomsets (LFA 7; Table S2) overlain by parallel-bedded, planar and trough cross-bedded pebble gravels and laminated coarse to medium sands, interpreted as aggrading gravel bars separated by shallow, sandy channels (LFA 1; Table S2), typical of shoal delta aggradation.

MSA 3 shoreline deposits

Shoreline lithofacies associations were observed in the south of the Brosna basin only, on the northern sides of the Birr

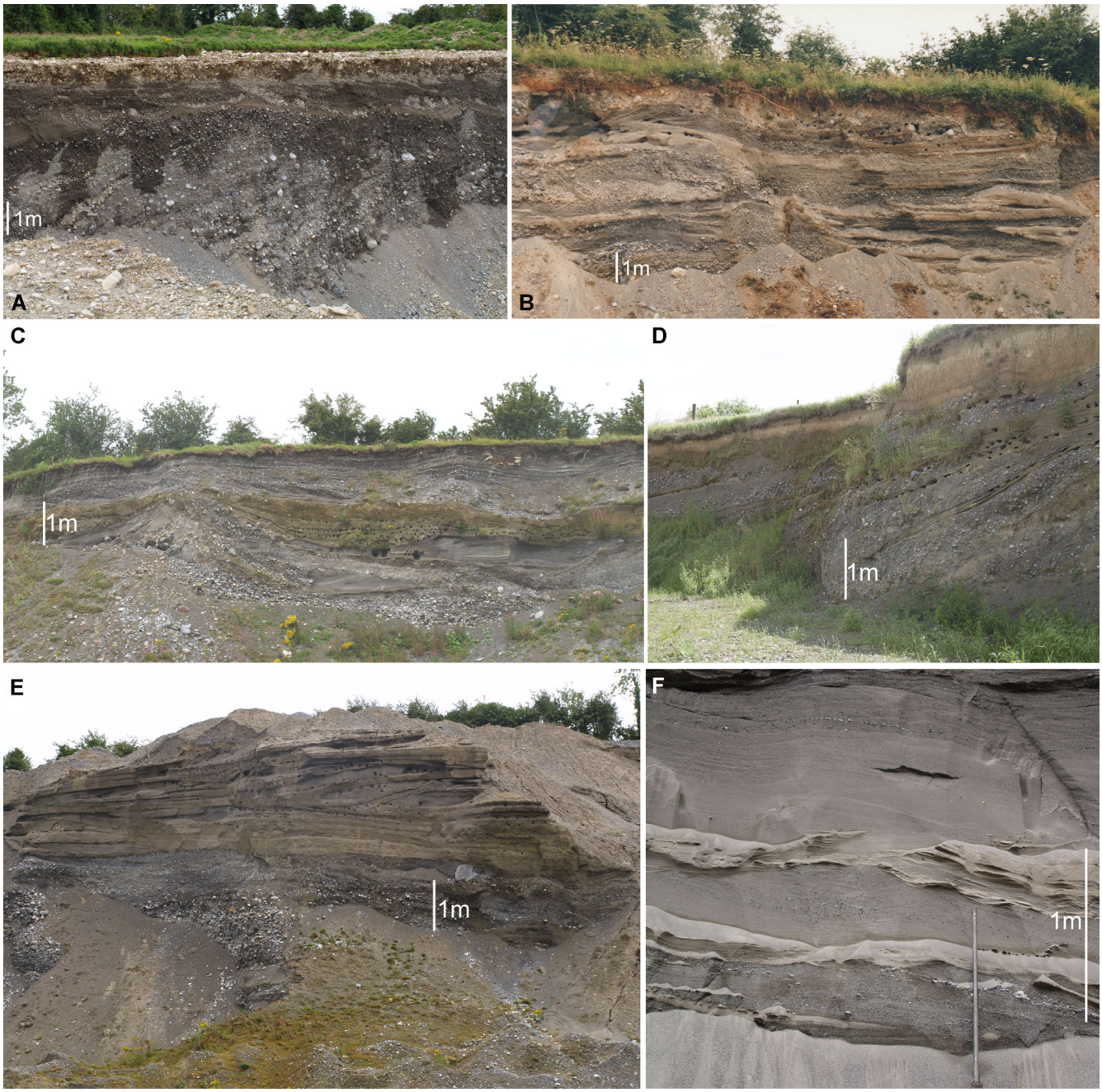

Figure 8. Exposures in lithofacies associations (LFAs) 1 to 4 (see Table S2). Location positions shown on Fig. 5. A. LFA 1 fluvial topsets consisting of Gh and Gp lithofacies overlying LFA 3 debris flow-dominated topsets, Gilbert-type delta, Location 5. B. LFA 1 fluvial sediments consisting of Gh and Gp lithofacies interbedded with Sh, and Sp lithofacies, shoal delta, Location 1. Exposure is transverse to the overall flow direction. C. A lower unit of LFA 1 fluvial sediments, partly distorted by ice push, overlain by a drape of LFA 7 distal subaqueous outwash consisting of Sr and Fl lithofacies, and capped by LFA 2 shoreline sediments consisting of Gp and Sp lithofacies overlain by laterally continuous Gh/Sh lithofacies, wave-dominated delta, Location 6. D. LFA 3 debris flow-dominated deltaic foresets, consisting of Gms and Gmg lithofacies, interbedded with Sn and Fl drapes, and capped by a drape of massive sandy silt interpreted as glaciolacustrine sediments, Gilbert-type delta, Location 4. E. Glaciofluvial conduit/channel sediments overlain by a thick drape of LFA 7 distal subaqueous outwash and then by LFA 4, density current-dominated foresets, wave-dominated delta, Location 6. F. LFA 4 density current-dominated foresets consisting of Ss, Sl and Sh lithofacies, with occasional Sr lithofacies, Gilbert-type delta, Location 10. [Color figure can be viewed at wileyonlinelibrary.com]

and Kilcormac eskers, where they are associated with a Type 2 kame cluster (Figs. 4, 6G). The sediments are characterised by an absence of silt compared with underlying and adjacent glaciofluvial deposits, indicating that they have been winnowed by wave action. Shoreline deposits most commonly occur as draped wedges of openwork, well-sorted, planar cross-bedded pebble and cobble gravels that occur along the side of the eskers in multiple small exposures along the sides of the main esker ridges (e.g. Fig. 9C, D). These sediments appear to be reworked from underlying glaciofluvial sediments.

At Location 16 a single, shallow, 60 m long exposure was also observed underlying the surface of a flat-topped kame (Table 1; Figs. 4, 6G). The kame is slightly raised along its northeastern margin, with a flat platform extending southwest from this area (Fig. 6G). The sediments consist of laterally continuous, thin beds of pebbles and granules with sand, with occasional thin sand beds (Fig. 9A, B). Individual sediment laminae and beds are well-sorted, but with rapid changes in particle size upward, and with occasional shape-sorting of coarser clasts. Occasional imbricated clasts indicate that transport was downslope. Bedding is usually conformable,

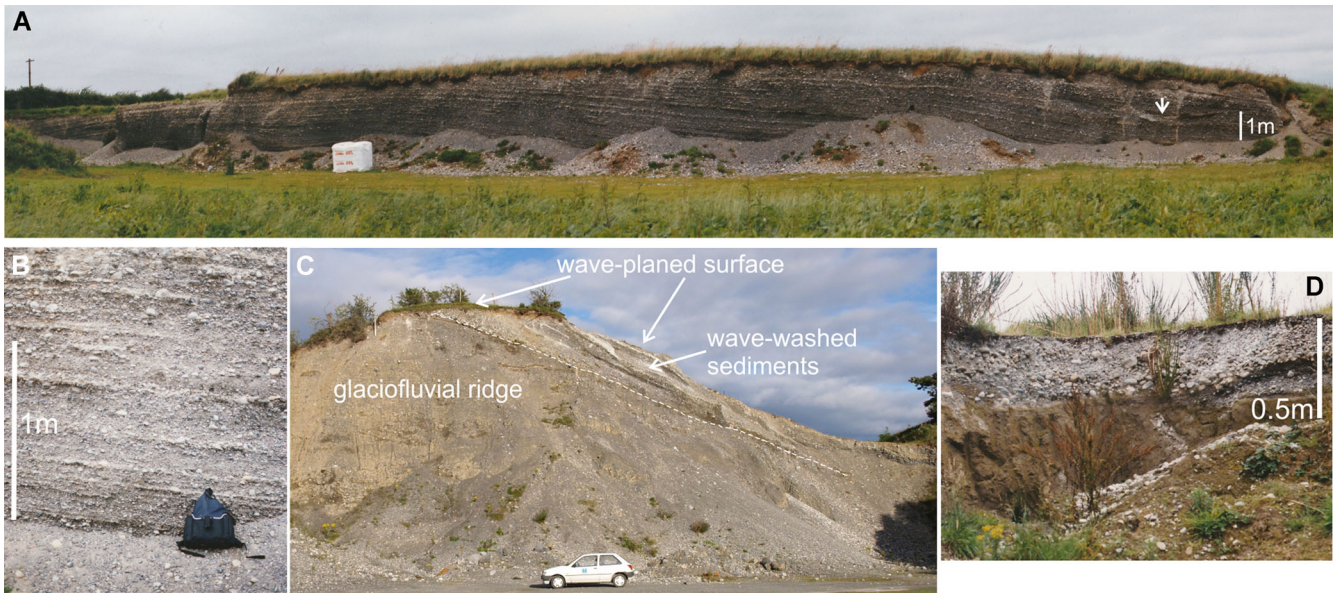

Figure 9. Exposures in lithofacies association (LFA) 2 shoreline sediments, southern Brosna Basin (see Table S2). Location positions shown on Fig. 5. A. LFA 2 shoreline sediments consisting of thinly bedded, well-sorted Gh and Sh lithofacies exhibiting changing dip along a 60 m long section, shoreline feature, Location 16. Arrow indicates a shallow scour. B. Close-up of sediments at Location 16. C. Location 18: Glaciofluvial ridge composed of conduit fill deposits, truncated along the southern margin and overlain by a wedge of planar cross-bedded, well-sorted, openwork and bimodal pebble and cobble gravels. The flattened surface of the esker and a terrace 1 m below the high point are interpreted as wave-planed terraces. Car for scale. D. Openwork, normally graded cross-beds of well-sorted pebble gravel overlying glaciolacustrine sediments, Location 17. [Color figure can be viewed at wileyonlinelibrary.com]

with occasional welded beds. However, a shallow scour 4–6 m wide and up to 30 m deep occurs toward the northeastern end of the exposure (white arrow on Fig. 9A). Dip of bedding changes along the exposure, giving a gently domed geometry to the deposit, partly mirrored in the kame surface, although the highest beds are truncated at the top and under the flat platform of the kame (LFA 2; Table S2; Figs. 5G, 9A). Dip angle is asymmetric with dips of 10–15° northeastward on the northeastern end of the exposure and up to 20° south-southeastward at the southwestern end.

The absence of fines and improved sorting compared with glaciofluvial sediments, the thin beds and rapid change in particle size, the relatively shallow angle of dip and the change in bed dip across the ridge is characteristic of formation as upper shoreface or beach sediments (Blair, 1999; Hiroki and Masuda, 2000; Mäkinen and Räsänen, 2003; Blair and McPherson, 2008). The scour at the northeastern end of the exposure may be a cut-and-fill structure, similar to those observed in upper shoreface sediments elsewhere (Pascucci *et al.*, 2009). The position of the exposure, at the landward end of a kame, and on the landward tip of a slightly raised area, indicates that the sediments may have formed part of a recurved gravel spit (e.g. Hiroki and Masuda, 2000). However, the detailed geomorphology is unclear, and parts of the deposit appear to have been truncated by further wave action.

MSA 4 subaqueous outwash fans

Subaqueous outwash fan deposits have been identified in the lowest parts of the Brosna and Suck basins between Lough Ree and Lough Derg, below 50 MOD (Fig. 4; Delaney 2001, 2002a). This is also the upper limit of fringing subaqueous outwash along eskers west of the Shannon. East of the Shannon, subaqueous outwash occurs up to 80 MOD, indicating higher water levels in this area. The subaqueous fans at Rooskagh (Location 26) and Monksland (Location 27) have been described previously (Delaney, 2001, 2002a) but the main features are summarised here for convenience. They occur at the downstream end of conduit fills and have a gently sloping surface, mirrored internally by the overall dip of bedding. Sediment size fines rapidly down-fan and upward through the fan from boulders to silt and clay, and there is a transition from super-critical to sub-critical tractional bedforms (LFAs 8, 9; Table S2; Fig. 10B, E) and then to suspension deposition (LFA 7; Fig. 10B). Infilled channels oriented parallel to the fan surface slope occur in mid- to distal fan sediments, a diagnostic feature of subaqueous outwash fans (Rust, 1977; Postma, 1983), and are formed by mass flows due to destabilisation of loosely packed material in response to a shock, such as an earthquake or iceberg calving event (Fig. 10C; Rust, 1977).

MSA 5 distal glaciolacustrine sediments

This MSA consists of flat or very low-relief areas underlain by Holocene wetland (raised bog and fen), lacustrine (calcareous marl) and alluvial sediments, which in turn overlie inorganic, massive and laminated silts and clays (Fig. 10D; LFA 10; Table S2). The lowest distal glaciolacustrine sediments are commonly rhythmically laminated and are interpreted as varved (Delaney, 2007). Later glaciolacustrine sediments are diffusely laminated or massive and contain sand (Long and O'Riordan, 2001; Delaney, 2007).

Deposits are thickest around modern lakes (Fig. 11). For example, at the southern end of Lough Ree, over 10 m of glaciolacustrine silt and clay underlies alluvium (Fig. 11A; Long and O'Riordan, 2001; Long, 2019) while the Lough Ennell basin contains glaciolacustrine deposits up to 14.5 m thick below Holocene sediments (Fig. 11B; Long, 2019). Elsewhere, Van der Meer and Warren (1997) record glaciolacustrine clays up to 5 m thick under Clara Bog, as do Carney *et al.* (2019) at Galros East, near Birr.

In the Suck basin over 3 m of glaciolacustrine sediments occur at Rooskagh (Fig. 10D; Delaney, 2007), while in the Inny basin extensive areas of peat also overlie glaciolacustrine sediments.

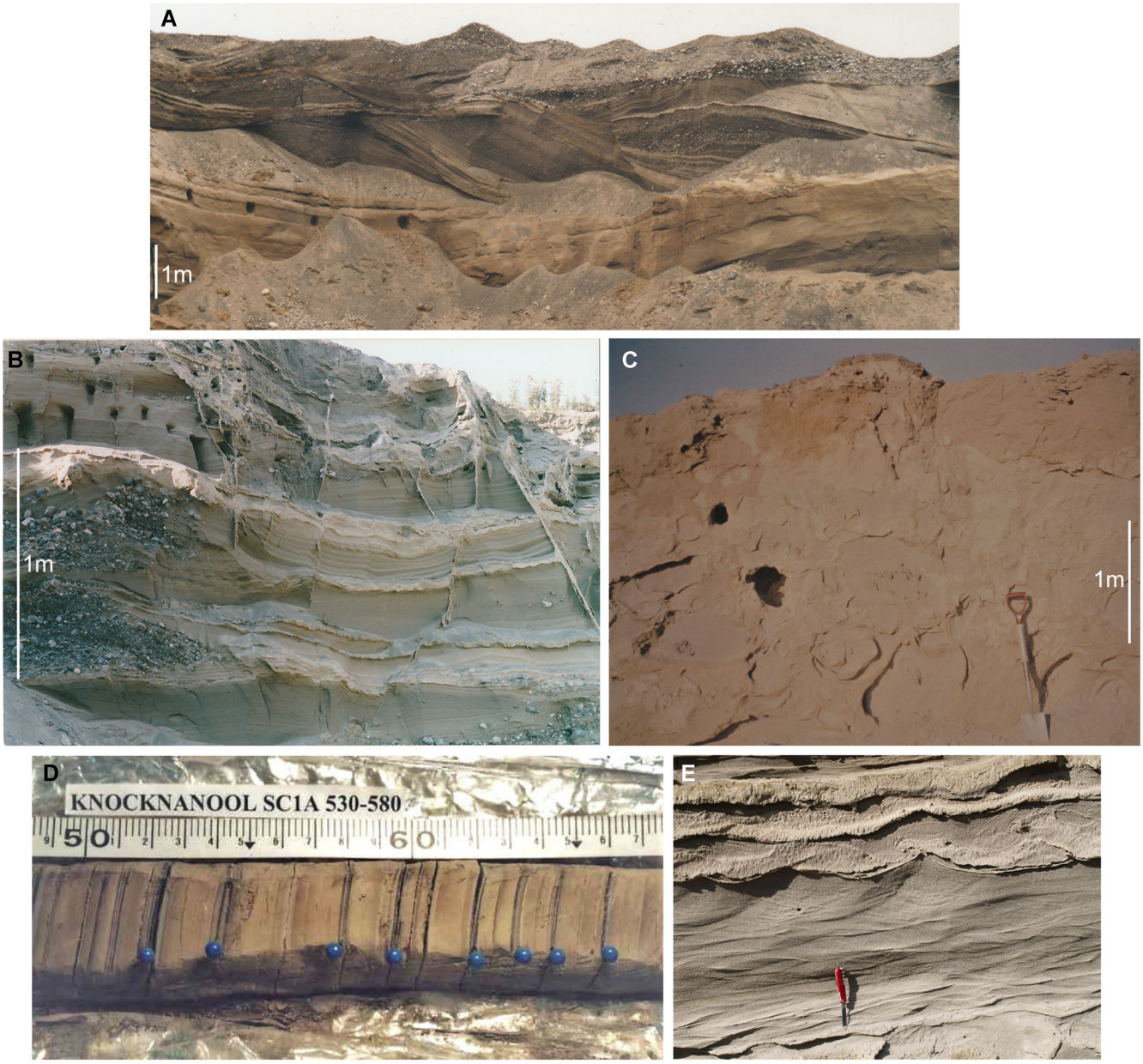

Figure 10. Sedimentary exposures in lithofacies associations (LFAs) 5 to 10 (see Table S2). Location positions shown on Fig. 5. A. LFA 5 stacked, convex-up foresets consisting of Sp pebbly sand foresets overlying LFA 7 distal subaqueous outwash, shoal delta, Location 1. B. LFA 6 toesets consisting of rhythmically bedded Ss, Sh and Sr lithofacies in medium sand, capped by drape-laminated silty sand (Fl lithofacies) with lenses of horizontally bedded bimodal gravels (Gh lithofacies), Gilbert-type delta, Location 4. C. LFA 9 subaqueous outwash fan mid-fan deposits. Channel infill consisting entirely of Ssd lithofacies including ball-and-pillow structures, Monksland fan, Location 28. E. LFA 10 distal glaciolacustrine sediments consisting of rhythmically laminated (varved) silt and clay. Paler summer layers composed of multiple normally graded units overlain by dark, thin silty clay winter units (indicated by blue pins), Location 27. F. LFA 7 distal subaqueous outwash sediments consisting of normally graded units showing a transition from A- to B-type climbing-ripple cross-lamination (Sr lithofacies) and then to drape-laminated silt (Fl lithofacies), Location 26. [Color figure can be viewed at wileyonlinelibrary.com]

Interpretation of landforms and deposits

Glaciofluvial/glaciolacustrine landforms and deposits

The largest landforms in this group are ice-contact deltas (MSAs 1, 2) and subaqueous outwash fans (MSA 4). These confirm that ice sheet-derived meltwater was discharging directly into standing water in all three basins. The resulting deposit type varies with land surface elevation, reflecting lake bathymetry, which in turn controlled basin storage capacity. Shoal deltas formed in shallow water near the watershed, during the earliest stages of lake development in the Brosna and Inny basins when water depths were insufficient for foreset development. Gilbert deltas formed at lower elevations as the ice margin retreated westward and northwestward along a reverse slope and water depth increased sufficiently to allow formation of debris flow-dominated foresets. In many deltas a change in foreset type laterally indicates increased distance from the sediment source and a shift from direct fluvial sediment input to remobilisation of material as hyperpycnal flows down the delta front from the upper part of the delta (Gobo *et al.*, 2014; Lang *et al.*, 2017; Winsemann *et al.*, 2018). Where lake bed elevations were lowest around the modern River Shannon (<50 MOD), subaqueous outwash fans (MSA 4) formed instead of deltas as deposition did not reach the water surface.

Most deltas are elongate parallel to ice flow direction (as indicated by subglacial lineations and moraine orientation), with steep side slopes, indicating deposition within an embayment in the ice margin. Embayments around conduit exits are common in modern water-terminating glaciers where

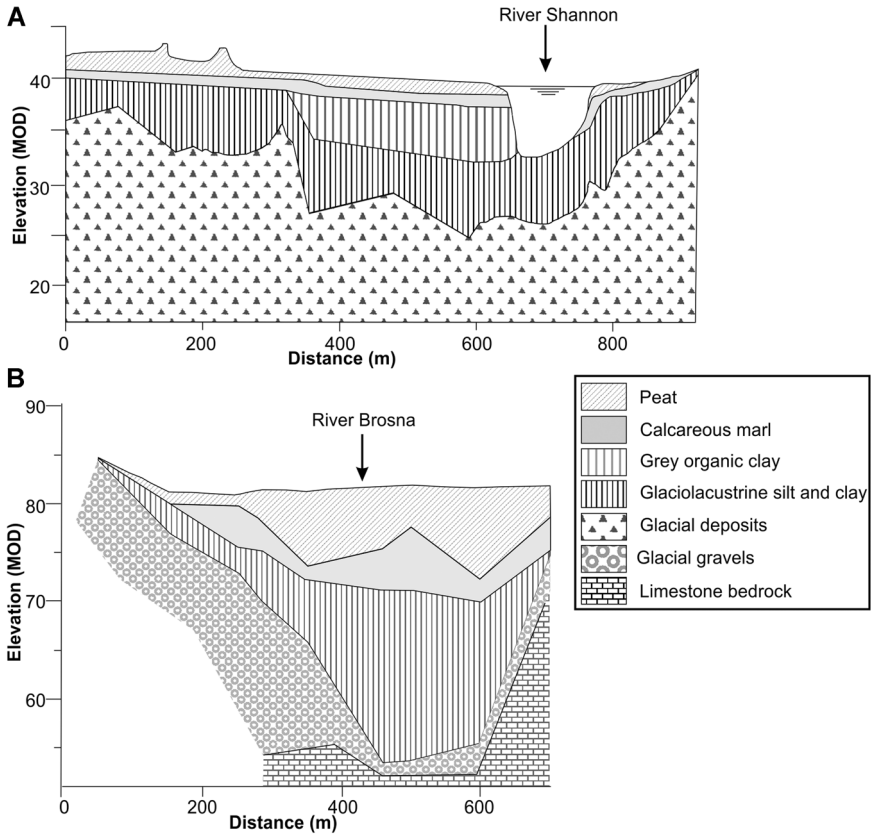

Figure 11. Cross-section of sedimentary sequence reconstructed from boreholes records. A. The Shannon flood plain north of Athlone. B. The Brosna floodplain north of Lough Ennell. Redrawn from Long (2019)

the glacier is grounded, and indicate enhanced retreat due to localised subaqueous melt, causing serac-type ice cliff failure through the melt season (e.g. Fried *et al.*, 2018; Bunce *et al.*, 2021). Gilbert deltas that extend parallel to the ice margin occur in the eastern part of the Brosna basin at Locations 4 and 7 (Fig. 4; Fig. 6E, F), and in the southwest at Location 10 (Fig. 4). This may reflect differences in ice dynamics in these areas as the deltas at Locations 4 and 10 formed after local ice margin oscillations (Delaney *et al.*, 2018; Delaney, 2019). The Location 7 delta may also have formed after an oscillation, as there is a marked shift in esker orientation from the ice-distal to the ice-proximal side of the delta (Fig. 4). These ice-margin oscillations likely involved advection of subglacial sediments toward the ice margin, providing material for delta formation (Boulton, 1996; Lønne and Nemec, 2011; Evans *et al.*, 2018). The deltas also have push moraines along their ice-contact margins, indicating sediment transfer (Evans *et al.*, 2018), while Location 4 and 10 deltas are linked to multiple eskers, indicating converging conduits and likely higher sediment input from meltwater discharge. Deltas extending parallel to the ice margin may thus indicate a temporary enhancement in sediment supply due to a local oscillation of the ice margin.

Shoreline features and sediments were observed along the southern and eastern margins of the Brosna basin only. Many of these features are associated with wave-planed surfaces. This localised distribution and concentration of such features likely reflects: 1) increased wave fetch within the proglacial lake in the Brosna basin as it expanded; and 2) longer exposure to wave action compared with the Inny and Suck basins, which were uncovered at a later stage of ice recession.

Subglacial lineations

Subglacial lineations provide some indication of ice-flow dynamics in the ice-sheet sub-marginal zone during the existence of Palaeolake Riada. Drumlins and MSGLs form part of a morphological continuum (Ely *et al.*, 2016) and indicate a wet-based ice sheet (e.g. Smith and Murray, 2009; King *et al.*, 2009; Iverson *et al.*, 2017). Increasing elongation of drumlins and MSGLS is controlled by a number of factors, including bed lithology, thickness of the deforming bed layer, basal shear stress, ice velocity and time (Greenwood and Clark, 2010; Barchyn *et al.*, 2016; Jamieson *et al.*, 2016). Where bed lithology is unchanged, as is the case here, a change in lineation length indicates a change in ice sheet basal conditions and ice dynamics. The occurrence of MSGLs obliquely overprinting drumlins around Lough Ree (Fig. 7) suggests a reduction in basal shear stress and an accompanying acceleration in ice velocity during this reoriented ice flow phase (Jamieson *et al.*, 2016).

Ice-flow transverse ridges

Small transverse ridges can form in a variety of ways, including as terrestrial ice-marginal ridges (e.g. Chandler *et al.*, 2016, 2020), as De Geer moraines at a grounded subaqueous margin (e.g. De Geer, 1940; Ojala, 2016), as subglacialc CSRs (e.g. Boulton *et al.*, 1996; Cline *et al.*, 2015), or supraglacial crevasse-fill ridges (e.g. Russell *et al.*, 2006; Evans *et al.*, 2012). Many ridges within the Brosna basin exhibit characteristics of ice-marginal moraines although some have characteristics of sub- or supraglacial crevasse infills (Delaney *et al.*, 2018). In the Inny basin, short ridges mapped by Meehan (1999) immediately south and east of Lough Sheelin contain traction and meltout tills consistent with ice-marginal formation as push or dump moraines. Moraines in the Suck basin are also at right angles to underlying lineations, indicating active ice margins orthogonal to preceding ice-flow directions. The ridges indicate that active ice occurred over large parts of the ice margin. In the Brosna basin, CSRs with underlying MSGLS indicate ice stagnation following an episode of accelerated ice flow and a dynamic sub-marginal ice zone (Delaney *et al.*, 2018).

Modelling the lake extent

Ice-margin position during lake expansion

Successive ice-margin positions are shown in Fig. 4, reconstructed using moraines and glaciofluvial features. In the Brosna basin, ice-margin orientation and ice-flow indicators indicate that the Eiscir Riada formed within an interlobate zone, in a conduit exiting into an embayment (Fig. 4; Pellicer *et al.*, 2012). North of the esker, successive groups of ice-flow transverse ridges indicate retreat of the ice margin northwestward from the Brosna basin into the Inny basin and the northern part of the Suck basin (Fig. 4). These ridge groups continue northeastward toward the Irish Sea coast, indicating that they formed contemporaneously with moraines around Dundalk Bay (see below).

South of the Eiscir Riada, ice recession was roughly westward in the eastern Brosna basin and southwestward in the southern part of that basin, forming a curved ice margin (Fig. 4). Around Birr, moraines and delta ice-contact faces indicate a shift to a northeast–southwest ice-margin orientation, with a corresponding change in esker orientation (Fig. 4). Minor moraines indicate that this margin swung to a north–south orientation northeastward and continued to the Esker Hill delta on the Eiscir Riada, (8, Fig. 4). This bulge in the ice margin is associated with a local oscillation (Fig. 16 in Delaney *et al.*, 2018).

Small groups of moraines lying above 60 MOD in the Suck basin (Fig. 4) indicate northwestward retreat in the northern part of the basin, similar to the Inny basin. Between the Suck River and Lough Derg, moraine groups indicate a north–south-aligned margin. South of Lough Derg, the reconstruction of Clark *et al.* (2012; Fig. 3) indicates that ice extended eastward and southeastward across Lough Derg, and into the lowlands around Nenagh (Figs. 1, 5). This margin is assumed to have retreated westward at a similar rate to the ice in the Suck basin.

Four ice-margin positions (numbered 1–4 on Fig. 4) were selected for further modelling, linked to likely maximum extents of specific outflows from the proglacial lake (see below).

Ice-margin ages and GIA model application

Ice margins north of the Eiscir Riada have been traced using minor moraines to the Irish Sea coast around Dundalk Bay, where they link to previously identified and dated ice-margin positions (McCabe *et al.*, 2007; Chiverrell *et al.*, 2013, 2018). This indicates that the earliest ice-margin position for Palaeolake Riada correlates with the Dunany Point readvance moraine, formed after 17.4 ka BP, while the youngest margin correlates with moraines on the north side of Dundalk Bay formed during ice retreat after 16 ka BP (Chiverrell *et al.*, 2013, 2018). Accordingly, the four ice-margin positions and associated extents of Palaeolake Riada were reconstructed using the GIA model for 17 ka BP (margin 1), 16.5 ka BP (margin 2) and 16 ka BP surfaces (margins 3 and 4, see below). A further model showing the lake extent after ice retreat used the GIA model for 15 ka BP.

Identification of lake outflows and relationship to glaciolacustrine features

Lake outflows for the selected ice margins were identified using the glacio-isostatically adjusted 25 m DEM for the relevant time period. Modern col elevations, together with elevations of glaciolacustrine features indicating water surface level, are plotted against distance from the Shannon Gorge entrance (the most southerly point of the lake; Fig. 12), to examine the impact of glacio-isostasy and confirm probable ice-margin positions.

Lake outflows in the Brosna basin

An outflow for the earliest lake stage (17 ka BP), identified by Pellicer *et al.* (2012), lies at 89 MOD at Derries, south of Kilbeggan (Figs. 4, 12) and correlates with local delta heights of 87–90 MOD (Table 1). Flow through this col drained south through the Barrow catchment to the Celtic Sea. Two further outflows near Daingean (east) and Geashill (south) at 83 and 84 MOD are at similar heights to delta surfaces along the northern basin margin, indicating that ice retreat occurred earlier north of the Eiscir Riada (Fig. 12; Table 1; Pellicer *et al.*, 2012).

West of Geashill, the lowest outflow, at Clonad, is at 80 MOD. This col is partly infilled by peat, indicating the true surface is lower, so the col is correlate with deltas at Locations 6–10 (73–78 MOD), and the highest terrace on the Kilcormac esker (Location 16; 76 MOD) (Fig. 12; Table 1). The wide distribution of features with elevations near the Clonad outflow elevation in the Brosna basin confirms that this was the main lake outflow until ice retreated sufficiently westward to uncover lower cols in the Inny basin or to the south. However, a number of surfaces intermediate in height between the Clonad col elevation and these lower cols indicate that lake level varied by up to 9 m during this stage, reflecting seasonal variation in lake level and/or the impact of subglacial or supraglacial lake drainage through the ice dam as the lake thinned.

Cols in the Inny basin

Meltwater channels and sand and gravel deposits, including a shoal delta (Location 24; Figs. 4, 12), indicate that small perched lakes formed along the southern margin of the Inny basin during early ice retreat, draining over the watershed into the Brosna and Boyne basins. As the ice margin retreated, water drained parallel to the ice margin through northeast–southwest-oriented meltwater channels that converged on lower elevation cols. These cols are mostly higher than the Brosna basin cols, even when lowered by GIA. However, when modelled GIA is applied, the Barbavilla col east of Lough Derravaragh (currently at 81 MOD; Fig. 12) is at a similar elevation to lower shoreline terraces in the Brosna basin and delta surfaces near Birr and in the Suck Basin (Locations 11, 12, 15, 16, 17 and 19; 66–69 MOD), indicating that the Inny basin col controlled lake level prior to the opening of cols around the southern end of Lough Derg. The opening of the Barbavilla col involved diversion of meltwater into the Boyne catchment and switching of meltwater discharge into the Irish Sea basin.

Outflows south of the Brosna basin

Southeast of Birr, the watershed extends southwestward from the Slieve Blooms along the Devils Bit and Keeper Hills, forming a topographic barrier to lake drainage (Fig. 1). Perched lakes developed along the northwestern margin of these hills during initial ice recession (Charlesworth, 1928) but cols are too high to have drained Palaeolake Riada. However, as ice recession continued, lateral meltwater channels diverted drainage southwestward to a col at Carrigatogher Bog (at 50 MOD today; modelled at 62 MOD at 16 ka), on the watershed between the Nenagh and Kilmastulla rivers (Fig. 1). This col then acted as the main drainage route for the Shannon basin while the Shannon Gorge was blocked with ice. After GIA, the

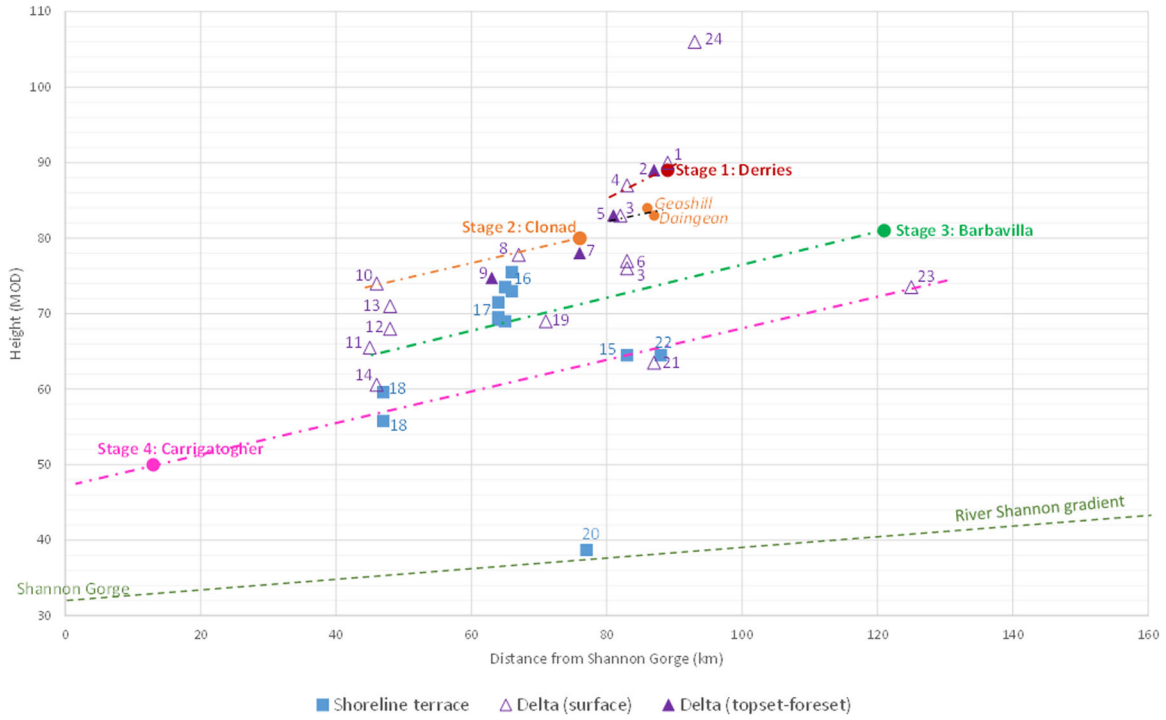

Figure 12. Graph showing relative elevations of lake-related features, plotted against distance from the Shannon Gorge. [Color figure can be viewed at wileyonlinelibrary.com]

Carrigatogher col remains lower than the Barbavilla col, but is at a similar height to the lowest shorelines and deltas in the Brosna basin (Locations 15, 18) and deltas in the Inny basin (Locations 21, 22). This indicates that the Carrigatogher col was the outflow from the ice-dammed lake during its last stage. As the Shannon estuary was still blocked by ice (Roberts *et al.*, 2020), water discharged southward via the Mulkear river valley.

Reconstructions of lake extent

The four modelled stages of the ice-dammed lake, at 17.0, 16.5 and 16.0 ka BP, are shown in Fig. 13.

Stage 1 (Derries outflow, 17 ka BP)

Margin 1 relates to the highest Brosna basin outflow at Derries (89–90 MOD) and is similar to Margin III of Pellicer *et al.* (2012; Figs. 12, 13A), with minor adjustment. The margin is correlated with the Dunany Point Moraine and modelled on the 17 ka BP GIA surface, forming as ice retreat from the Killard Point Stadial maximum advance began. At this stage, lake extent was 82 km^2, with an average water depth of 13.5 m and a 27 km long subaqueous margin (Table 2). The lake occupied a v-shaped interlobate embayment, with the conduit in which the Eiscir Riada was forming at its apex (Fig. 13A).

Stage 2 (Clonad outflow, 16.5 ka BP)

Stage 2 represents the most westerly position of the ice margin while the lake still drained eastward from the Brosna basin (Fig. 13B) and was modelled using the 16.5ka BP GIA surface. By now the lake area had expanded to 850 km^2, with an 85 km long subaqueous margin and average water depth of 18.6 m, with depths of over 30 m along the margin between the Eiscir Riada and Lough Ree. Deltas were forming in front of several conduit exits (Fig. 4). Ice recession was most pronounced around the Eiscir Riada, the configuration of which indicates that two closely spaced conduits drained contemporaneously in the interlobate zone. North of this esker the margin was relatively linear; to the south the margin bulged after local readvance due to ice-marginal surging behaviour around Birr (Delaney *et al.*, 2018; Delaney, 2019). The lake was now over 90 km long and extended southward beyond Birr and northeastward into the Lough Ennell basin. Wave-planed terraces and associated shoreline features were forming in the eastern and southern Brosna basin.

Stage 3 (Barbavilla outflow, 16.5 ka BP)

With continued ice-marginal recession west and northwestward across the Inny and Suck basins, the Barbavilla outflow opened (Fig. 13C). The timing of the retreat is uncertain, so the 16.5 ka BP GIA surface was used to model this stage. The Barbavilla col opening diverted meltwater drainage eastward into the Boyne catchment and the Irish Sea basin, and Palaeolake Riada water level dropped by approximately 4 m. As retreat continued, the lake increased in area to 2112 km^2, with a volume of 47.9 km^3, a subaqueous margin of 113 km, and an average water depth of 22.7 m. The deepest waters were in the southern Lough Ree basin, where the modern Suck and Shannon flood plains intersect the ice margin, and at the northern end of Lough Derg. Within the palaeolake, islands emerged and the reconstruction indicates that Lough Ennell had become separated from the main lake. In the southern Brosna basin, the surface of many features were wave-planed to this level (Locations 11, 12, 17), as ice had retreated from this area. Multiple flat-topped landforms in the Inny basin have surfaces at this elevation and are also likely to have been wave-planed (Delaney, 2002b).

Stage 4 (Carrigatogher outflow, 16 ka BP)

This lake stage is modelled on the 16 ka BP GIA surface, and formed when ice recession westward uncovered the Carrigatogher Bog col (50 MOD; Fig. 13D). Although the lake area is the largest modelled, at 2358 km^2, average lake depth was

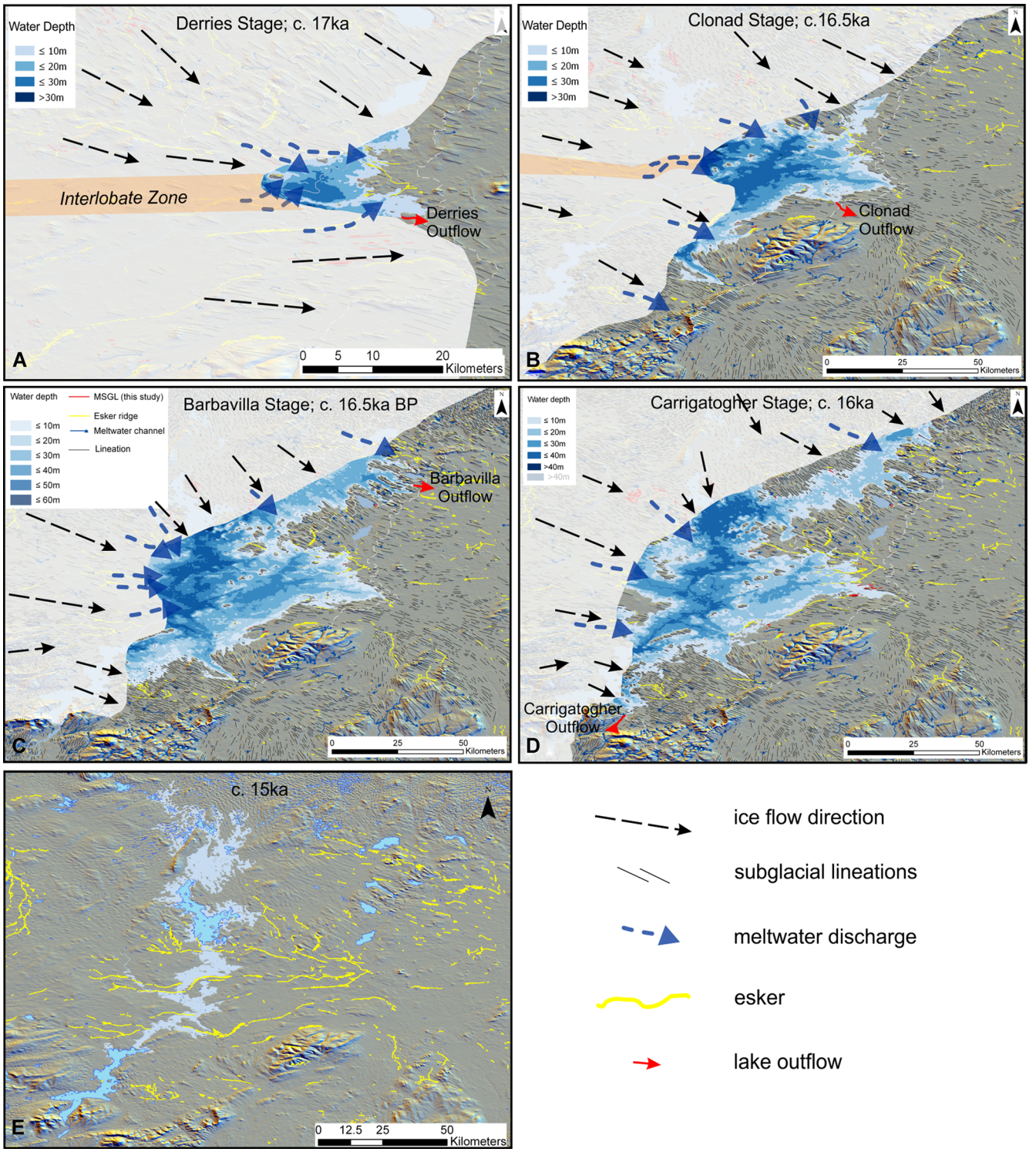

Figure 13. Models of Palaeolake Riada and the adjacent ice sheet, showing expansion of the lake as ice receded. [Color figure can be viewed at wileyonlinelibrary.com]

Table 2. Characteristics of Palaeolake Riada at each stage.

Lake outflow	Area	Volume	Maximum water depth (plus modern lake depth)	Average water depth	Outflow height at 16 ka BP (MOD)
Derries (17 ka BP)	82 km^2	1.117 km^3	33 m	13.5 m	81
Clonad (16.5 ka BP)	850 km^2	15.795 km^3	47 m	18.6 m	75
Barbavilla (16 ka BP)	2112 km^2	47.90 km^3	66 m (101 m)	22.7 m	71
Carrickatogher (16 ka BP)	2358 km^2	38.185 km^3	45 m (80 m)	16.2 m	62
Shannon Gorge (15 ka BP)	888 km^2	4.453 km^3	17 m (53 m)	5 m (outside modern lakes)	38

reduced to 16.2 m, with maximum depths of around 66 m in the Lough Ree basin. Water volume was just over 38 km^3, and the subaqueous margin was under 90 km long, as the lake level dropped by 9 m during the opening of the Carrigatogher col. Meltwater now drained southward through the Killmastulla river valley to ultimately discharge into the Celtic Sea.

Stage 5 (ice-free, 15 ka BP)

The final lake extent is shown after the opening of the Shannon Gorge below Lough Derg and the 15 ka BP GIA model, as ice is thought to have receded west of the Shannon by then (Roberts *et al.*, 2020). The opening of the gorge resulted in a 14 m drop in water level, and a considerable reduction in lake area and volume (Fig. 13E).

Discussion

The analysis of glaciolacustrine landforms and sediments presented here confirms that an extensive ice-dammed lake formed along the margin of the last IIS in the central Irish midlands, as it receded down a reverse slope toward the Shannon River between 16 and 17 ka BP. The lake extent was primarily controlled by the location of ice dams. However, glacio-isostasy also had an impact on the lake area and the location of outflows, and a large lake continued to exist between Lough Derg and Lough Ree into the Holocene.

At its largest, ice-dammed Palaeolake Riada extended over 2300 km^2, nearly 3% of the island of Ireland, and had a water-terminating ice margin of almost 115 km^2. This is an order of magnitude larger than the largest ice-dammed lakes in currently glaciated regions (Schomacker, 2010; Shugar *et al.*, 2020; How *et al.*, 2021) and considerably larger than other ice-dammed lakes that formed during the Last Glacial Termination in Ireland; for example, Glacial Lough Neagh covered <500 km^2 (Charlesworth, 1939) and Glacial Lake Blessington 84 km^2 (Synge *et al.*, 1975). However, Palaeolake Riada was smaller than the largest proglacial lake in the British Isles, Glacial Lake Humber/Fenland (area >12 000 km^3, volume 257 km^3; Clark *et al.*, 2004; Murton and Murton, 2012; *Clark et al.*, 2018), and much smaller than the largest lakes that formed along the margins of the last Laurentide and Eurasian ice sheets (e.g. Teller and Leverington, 2004). Nevertheless, the presence of such an extensive water body is likely to have had a significant impact on ice recession and associated ice dynamics during IIS recession across the Irish midlands given the long water–ice contact margin that existed. Studies of modern freshwater-terminating glaciers indicate that retreat rates are likely to have been intermediate between marine-terminating and land-terminating ice margins at that time (Warren and Kirkbride, 2003; Benn *et al.*, 2007), and that recession of this part of the ice sheet is likely to have been partly decoupled from climate (Benn *et al.*, 2007; Sutherland *et al.*, 2020).

Reconstruction of multiple stages in the evolution of Palaeolake Riada provides an opportunity to examine changes in ice–lake interactions through time. In modern ice–contact lakes ice recession occurs by a combination of thermo-mechanical processes, including surface, waterline and submarine melting, calving by serac fall and buoyancy calving (e.g. Benn *et al.*, 2007). The relative importance of any ablation process is dependent on a combination of factors, including the length of the ice–lake contact margin (Warren and Kirkbride, 2003; Benn *et al.*, 2007; Tsutaki *et al.*, 2019), the ratio between water depth and ice thickness (Warren and Kirkbride, 2003; Slater *et al.*, 2021), air and water temperature, the location of meltwater discharge outlets along the ice margin (e.g. Schild *et al.*, 2018; Fried *et al.*, 2019; How *et al.*, 2019), and structural features near the ice margin (e.g. Dell *et al.*, 2019).

The impact of some of these features and variables can be inferred from the palaeolake reconstructions. During retreat across the Brosna basin, the development of an indented margin reflects both the impact of discharge outlet location and variance in the water depth:ice thickness ratio. At this stage, the highest recession rates occurred where deeper water, thinner ice associated with an ice interlobate zone, and two large discharge outlets combined to enhance ice removal at the margin. This is consistent with observations at modern marine tidewater glaciers that indicate that thermal undercutting of the ice face is enhanced around subglacial discharge outlets due to upwelling of low-density freshwater plumes that increase circulation of warmer water along the ice front (Schild *et al.*, 2018; Fried *et al.*, 2019; How *et al.*, 2019). However, this effect has been considered unimportant at freshwater-terminating ice margins as meltwater discharges are colder and denser than lake water, preventing plume upwelling (e.g. Sugiyama *et al.*, 2016). In Palaeolake Riada, the thinner ice and lower flow velocities that occur in interlobate zones may have been more significant than water temperatures in controlling ice recession rates, altering the relationship between the ice flux to the margin and ice ablation (Benn *et al.*, 2007; Tsutaki *et al.*, 2019). Thin ice is also associated with conduit roof collapse and enhanced recession around the conduit mouth (e.g. Egli *et al.*, 2021).

The impact of the interlobate zone characteristics on recession rates decreased as the ice recession continued west into the Suck and Inny basins, with a northward shift in the region of most rapid ice-margin recession toward the deepest part of the basin (water depths up to 100 m), reflecting the impact of lake bathymetry and associated increases in ice-marginal buoyancy and ice calving (Warren, 1994; Warren and Kirkbride, 2003). This change to a relatively smoothed ice margin west of the Shannon River may also reflect the increased impact of ice-marginal buoyancy, combined with waterline and near surface thermal erosion, on ice recession across the entire subaqueous ice margin, as the lake area expanded and the larger area of water surface absorbed more heat in summer, allowing water temperatures to rise and enhancing melting along the ice front (Kirkbride and Warren, 1997; Warren and Kirkbride, 2003; Sugiyama *et al.*, 2016). The increased wave fetch also likely increased mechanical erosion along the subaqueous margin. Further south, ice recession rates were lower as the lake expanded across higher elevation terrain east of Lough Derg and ice-marginal buoyancy and calving reduced in the shallower waters there. This lower recession rate likely prevented ablation of the ice dam in this area.

The expanding ice-contact lake also appears to have affected ice-flow dynamics near the ice margin, most evidently around Lough Ree, where there is evidence for ice-flow deflection and accelerated ice flow southward and toward deeper water in the lake basin (Fig. 7). Such shifts in ice-flow velocity and direction are known from modern proglacial lakes (e.g. Storrar *et al.*, 2017; Dell *et al.*, 2019; Tsutaki *et al.*, 2019; Baurley *et al.*, 2020) and reflect an increase in subglacial water pressure, reduced basal drag and increased longitudinal strain rates and ice-flow velocity where deeper water occurs at the ice margin (Benn *et al.*, 2007; Tsutaki *et al.*, 2019). This reorganisation may also have caused local readvances of the ice margin, such as those recorded at Birr and Clavin's Hill. Another possibility is that the readvances were caused by ice margin debuttressing due to a reduction in water depth

(Kellerer-Pirklbauer *et al*., 2021), as the outflows at Barbavilla (for Birr) and Carrigatogher (for Lough Ree) opened. However, in the absence of reliable dating, this relationship cannot be tested.

Recent attempts at computer-based modelling of the evolution of the British–Irish Ice Sheet have succeeded in simulating the marine margins of the ice sheet well, but have only limited success in modelling terrestrial margins, particularly during the later recession of the IIS (e.g. Hubbard *et al*., 2009; Gandy *et al*., 2019). The work presented here indicates that this reflects a poor understanding of the controls on ice recession rates across Ireland during the Last Glacial Termination and that much work remains to be done in reconstructing those margins. In addition, modelling the impact of proglacial lakes on ice-sheet behaviour is likely to considerably improve simulations of ice recession and provide considerable information on the relationship between ice-sheet dynamics and climatic and non-climatic controls on recession.

Conclusions

This paper presents new geomorphological and sedimentological evidence for the development of ice-contact, proglacial Palaeolake Riada, which formed in the Irish midlands during recession of the terrestrial margin of the last IIS after the Killard Point Stadial, *c*. 17 ka BP. Ice-proximal deposition in the lake was dominated by glaciofluvial inputs and sediment characteristics were controlled by water depth, with shoal and Gilbert-type deltas and subaqueous outwash fans indicating increasingly deep water along the ice margin as it retreated west toward the Shannon. Laterally continuous shoreline terraces and associated shoreface deposits formed along the southeastern margin of the Brosna basin as the lake expanded westward, as this shoreline was exposed to wave action for the longest period during the lake's existence.

Changes in elevation of features whose surface formation was controlled by the water surface level indicate that post-glacial isostatic rebound has had a differential impact on feature elevation parallel to the known isostatic rebound (southwest to northeast across the island). After application of a GIA model, the correlation between water-controlled surfaces indicates at least four different water-surface elevations, corresponding to four different outflows, occurred, resulting in four falls in surface elevation as ice retreated west and northwest and the lake expanded. The lake was at its greatest volume during Stage 3, when the lake drained northeastward through the Barbavilla outflow, but at its greatest areal extent during Stage 4, when it drained southward through the Carrigatogher outflow, near the Shannon estuary.

Reconstruction of the ice margin configuration indicates that initially ice retreat was highest around an interlobate zone, where thinner ice, deeper water and the presence of discharge outlets enhanced retreat, but as the lake expanded a smoother margin developed, reflecting thermo-mechanical erosion across the entire subaqueous ice front.

The subaqueous margin also affected ice-flow dynamics, causing a shift in ice flow direction toward the deeper water along the margin. The presence of such an extensive ice-flow margin is also likely to have impacted overall recession rates, and should be considered in future modelling of the IIS.

Acknowledgements. The author thanks Kathryn Adamson and Matthew Carney for constructive discussions that contributed to the paper. Thanks also to Sarah Bradley for kindly supplying the glacio-isostatic adjustment model used for the research. The author acknowledges the extremely helpful reviews of two anonymous reviewers.

Supporting information

Additional supporting information can be found in the online version of this article.This article includes online-only Supplemental Data.

Table S1. Lithofacies codes used in recording sediments.

Table S2. Lithofacies Associations.

References

Alexander J, Bridge JS, Cheel J *et al*. 2001. Bedforms and associated sedimentary structures formed under supercritical water flows over aggrading sand beds. *Sedimentology* **48**: 133–152.

ASF DAAC. 2015. ALOS PALSAR_Radiometric_Terrain_Corrected_low_res; Includes Material © JAXA/METI 2007. Accessed through ASF DAAC 11 March 2019.

Ashley GM. 1975. Rhythmic sedimentation in glacial lake Hitchcock, Massachusetts-Connecticut. *SEPM Special Publications* **23**: 304–320.

Ashley GM. 1995. Glaciolacustrine environments. In *Glacial Environments, Volume 1: Modern Glacial Environments: Processes, Dynamics and Sediments*, Menzies J (ed). Butterworth-Heinemann: Oxford; 417–444.

Ashley GM, Southard JB, Boothroyd JC. 1982. Deposition of climbing-ripple beds: a flume simulation. *Sedimentology* **29**: 67–79.

Barchyn TE, Dowling TPF, Stokes CR *et al*. 2016. Subglacial bed form morphology controlled by ice speed and sediment thickness. *Geophysical Research Letters* **43**(14): 7572–7580.

Bateman MD, Evans DJA, Buckland PC *et al*. 2018. Last glacial dynamics of the Vale of York and North Sea lobes of the British and Irish ice sheet. *Proceedings of the Geologists' Association* **126**(6): 712–730.

Baurley NR, Robson BA, Hart JK. 2020. Long-term impact of the proglacial lake Jökulsárlón on the flow velocity and stability of Breiðamerkurjökull glacier, Iceland. *Earth Surface Processes and Landforms* **15**: 2647–2663.

Benn DI, Warren CR, Mottram RH. 2007. Calving processes and the dynamics of calving glaciers. *Earth-Science Reviews* **82**: 143–179.

Blair TC. 1999. Sedimentology of gravelly Lake Lahontan highstand shoreline deposits, Churchill Butte, Nevada, USA. *Sedimentary Geology* **123**: 199–218.

Blair TC, McPherson JG. 2008. Quaternary sedimentology of the Rose Creek fan delta, Walker Lake, Nevada, USA, and implications to fan-delta facies models. *Sedimentology* **55**(3): 579–615.

Bluck BJ. 2011. Structure of gravel beaches and their relationship to tidal range. *Sedimentology* **58**: 994–1006.

Boulton GS. 1996. Theory of glacial erosion, transport and deposition as a consequence of subglacial sediment deformation. *Journal of Glaciology* **42**(140): 43–62.

Boulton GS, van der Meer JJM, Hart JK *et al*. 1996. Till and moraine emplacement in a deforming bed surge – an example from a marine environment. *Quaternary Science Reviews* **15**: 961–988.

Bradley SL, Milne GA, Shennan I *et al*. 2011. An improved Glacial Isostatic Adjustment model for the British Isles. *Journal of Quaternary Science* **26**(5): 541–552.

Brennand TA. 1994. Macroforms, large bedforms and rhythmic sedimentary sequences in subglacial eskers, south-central Ontario: implications for esker genesis and meltwater regime. *Sedimentary Geology* **91**: 9–55.

Buckel J, Otto JC, Prasicek G *et al*. 2018. Glacial lakes in Austria – distribution and formation since the Little Ice Age. *Global and Planetary Change* **164**: 39–51.

Bunce C, Nienow P, Sole A *et al*. 2021. Influence of glacier runoff and near-terminus subglacial hydrology on frontal ablation at a large Greenlandic tidewater glacier. *Journal of Glaciology* **67**(262): 343–352.

Burke MJ, Woodward J, Russell AJ *et al*. 2008. Controls on the sedimentary architecture of a single event englacial esker: Skeidarárjökull, Iceland. *Quaternary Science Reviews* **27**: 1829–1847.

Carling PA. 1996. Morphology, sedimentology and palaeo-hydraulic significance of large gravel dunes: Altai Mountains, Siberia. *Sedimentology* **43**: 647–664.

Carney M, Delaney C, Adamson K. 2019. Location 3: sediments from Glacial Lake Riada. In *Glacial deposits in the Irish Midlands. INQUA 2019 Field Guide M:GL-5*, Delaney C (ed). Irish Quaternary Association: Dublin; 48–53.

Carrivick JL, Quincey DJ. 2014. Progressive increase in number and volume of ice-marginal lakes on the western margin of the Greenland Ice Sheet. *Global and Planetary Change* **116**: 156–163.

Carrivick JL, Tweed FS. 2013. Proglacial lakes: character, behaviour and geological importance. *Quaternary Science Reviews* **78**: 34–52.

Chandler BMP, Evans DJA, Roberts DH. 2016. Characteristics of recessional moraines at a temperate glacier in SE Iceland: insights into patterns, rates and drivers of glacier retreat. *Quaternary Science Reviews* **135**: 171–205.

Chandler BMP, Chandler SJP, Evans DJA *et al*. 2020. Sub-annual moraine formation at an active temperate Icelandic glacier. *Earth Surface Processes and Landforms* **45**(7): 1622–1643.

Charlesworth JK. 1928. The glacial retreat from central and southern Ireland. *Quarterly Journal of the Geological Society London* **84**: 295–300.

Charlesworth JK. 1939. Observations on the glaciation of north-east Ireland. *Proceedings of the Royal Irish Academy, Section B* **45**: 255–295.

Charlesworth, JK. 1963. Some observations on the Irish Pleistocene. *Proceedings of the Royal Irish Academy, Section B* **62**: 295–322.

Chiverrell RC, Thrasher IM, Thomas GSP *et al*. 2013. Bayesian modelling the retreat of the Irish Sea Ice Stream. *Journal of Quaternary Science* **28**: 200–209.

Chiverrell RC, Smedley RK, Small D *et al*. 2018. Ice margin oscillations during deglaciation of the northern Irish Sea Basin. *Journal of Quaternary Science* **33**: 739–762.

Chiverrell RC, Thomas GSP, Burke M *et al*. 2020. The evolution of the terrestrial-terminating Irish Sea glacier during the last glaciation. *Journal of Quaternary Science* **36**(5): 752–779.

Clark CD, Ely JC, Greenwood SL et al. 2018. BRITICE Glacial Map, Version 2: A map and GIS database of glacial landforms of the last British-Irish Ice Sheet. *Boreas* **47**: 11–27.

Clark CD, Evans DJA, Khatwa A *et al*. 2004. Map and GIS database of glacial landforms and features related to the last British Ice Sheet. *Boreas* **33**: 359–375.

Clark CD, Hughes ALC, Greenwood SL *et al*. 2012. Pattern and timing of retreat of the last British-Irish Ice Sheet. *Quaternary Science Reviews* **44**: 112–146.

Clark CD, Chiverrell RC, Fabel D *et al*. 2021. Timing, pace and controls on ice sheet retreat: an introduction to the BRITICE-CHRONO transect reconstructions of the British-Irish ice sheet. *Journal of Quaternary Science* **36**(5): 673–680.

Cline MD, Iverson NR, Harding C. 2015. Origin of washboard moraines of the Des Moines Lobe: spatial analyses with LiDAR data. *Geomorphology* **246**: 570–578.

Cockburn JMH, Lamoureux SF. 2008. Inflow and lake controls on short-term mass accumulation and sedimentary particle size in a High Arctic lake: implications for interpreting varved lacustrine sedimentary records. *Journal of Paleolimnology* **40**: 923–942.

Dardis GF. 1986. Late Pleistocene Glacial lakes in South-Central Ulster, Northern Ireland. *Irish Journal of Earth Sciences* **7**(2): 133–144.

De Geer G. 1940. *Geochronologia Suecica Principles*. 18, Kungliga Svenska Vetenskapsakademiens Handlingar III.

Delaney CA. 2001. Morphology and sedimentology of the Rooskagh esker, Co. Roscommon. Irish *Journal of Earth Sciences* **19**: 12–21.

Delaney CA. 2002a. Sedimentology of a glaciofluvial landsystem, Lough Ree area, Central Ireland: implications for ice margin characteristics during Devensian deglaciation. *Sedimentary Geology* **149**: 111–126.

Delaney CA. 2002b. Esker formation and the nature of deglaciation: the Ballymahon esker, central Ireland. *North West Geography* **1**(2): 22–33.

Delaney CA. 2007. Seasonal controls on deposition of Late Devensian glaciolacustrine sediments, central Ireland. In *Glacial Sedimentary Processes and Products. Special Publication of the International Association of Sedimentologists, 39*, Hambrey MJ, Christofferson P, Glasser NP *et al*. (eds). Blackwells: Oxford; 149–163.

Delaney C. 2019. *Glacial deposits in the Irish Midlands. INQUA 2019 Field Guide M:GL-5*. Irish Quaternary Association: Dublin.

Delaney C, McCarron S, Davis S. 2018. Irish Ice Sheet dynamics during deglaciation of the central Irish Midlands: evidence of ice streaming and surging from airborne LiDAR. *Geomorphology* **306**: 235–253.

Dell R, Carr R, Phillips E *et al*. 2019. Response of glacier flow and structure to proglacial lake development and climate at Fjallsjökull, south-east Iceland. *Journal of Glaciology* **65**(250): 321–336.

Edwards R, Craven K. 2017. Relative sea-level change around the Irish Coast. In *Advances in Irish Quaternary Studies*, Coxon P, McCarron S, Mitchell F (eds). Atlantis Press, 181–215.

Egli PE, Belotti B, Ouvry B *et al*. 2021. Subglacial channels, climate warming, and increasing frequency of Alpine glacier snout collapse. *Geophysical Research Letters* **48**: e2021GL096031.

Eilertsen R, Corner GD, Aasheim O *et al*. 2011. Facies characteristics and architecture related to palaeodepth of Holocene fjord-delta sediments. *Sedimentology* **58**: 1784–1809.

Ely JC, Clark CD, Spagnolo M *et al*. 2016. Do subglacial bedforms comprise a size and shape continuum? *Geomorphology* **257**: 108–119.

Emery AR, Hodgson DM, Barlow NLM *et al*. 2019. Left high and dry: deglaciation of the Dogger Bank, North Sea, recorded in proglacial lake evolution. *Frontiers in Earth Science* **7**: 234.

Evans DJA, Benn DI. 2004. A practical guide to the study of glacial sediments, *Arnold*. London.

Evans DJA, Strzelecki M, Milledge DG *et al*. 2012. Hørbyebreen polythermal glacial landsystem, Svalbard. *Journal of Maps* **8**(2): 146–156.

Evans DJA, Roberts DH, Hiemstra JF *et al*. 2018. Submarginal debris transport and till formation in active temperate glacier systems: the southeast Iceland type locality. *Quaternary Science Reviews* **195**: 72–108.

Farrington A. 1957. Glacial Lake Blessington. *Irish Geography* **3**: 216–222.

Farrington A, Synge FM. 1970. The eskers of the Tullamore district. In *Irish Geographical Studies in Honour of E. Estyn Evans*, Stephens N, Glasscock RE (eds). Queens University: Belfast; 49–52.

Flint RF. 1930. The origin of the Irish "eskers". *Geographical Review* **20**(4): 615–630.

Fried MJ, Catania GA, Stearns LA *et al*. 2018. Reconciling drivers of seasonal terminus advance and retreat at 13 central west Greenland tidewater glaciers. *Journal of Geophysical Research, Earth Surface* **123**(1590): 1607.

Fried MJ, Carroll D, Catania GA *et al*. 2019. Distinct frontal ablation processes drive heterogeneous submarine terminus morphology. *Geophysical Research Letters* **46**: 12083–12091.

Gallagher C, Thorp M, Steenson P. 1996. Glacier dynamics around Slieve Bloom, Central Ireland. *Irish Geography* **29**(2): 67–82.

Gandy N, Gregoire LJ, Ely JC *et al*. 2019. Exploring the ingredients required to successfully model the placement, generation and evolution of ice streams in the British-Irish Ice Sheet. *Quaternary Science Reviews* **223**: 105915.

Gilbert GK. 1885. The topographic features of lake shores. *U.S. Geological Survey Annual Report* **5**: 69–123.

Gobo K, Ghinassi M, Nemec W. 2014. Reciprocal changes in foreset to bottomset facies in a Gilbert-type delta: response to short-term changes in base level. *Journal of Sedimentary Research* **84**: 1079–1095.

Gobo K, Ghinassi M, Nemec W. 2015. Gilbert-type deltas recording short-term base-level changes: delta-brink morphodynamics and related foreset facies. *Sedimentology* **62**: 1923–1949.

Greenwood SL, Clark CD. 2008. Subglacial bedforms of the Irish Ice Sheet. *Journal of Maps* **4**(1): 332–357.

Greenwood SL, Clark CD. 2009a. Reconstructing the last Irish Ice Sheet 1: changing flow geometries and ice flow dynamics deciphered from the glacial landform record. *Quaternary Science Reviews* **28**: 3085–3100.

Greenwood SL, Clark CD. 2009b. Reconstructing the last Irish Ice Sheet 2: a geomorphologically-driven model of ice sheet growth, retreat and dynamics. *Quaternary Science Reviews* **28**: 3101–3123.

Greenwood SL, Clark CD. 2010. The sensitivity of subglacial bedform size and distribution to substrate lithological control. *Sedimentary Geology* **232**: 130–144.
Geological Survey of Ireland. 2017. Quaternary Sediments and Geomorphology. Open Access dataset, 2017. Available at: http://www.gsi.ie/Mapping.htm (last accessed July 2017).
Hiroki Y, Masuda F. 2000. Gravelly spit deposits in a transgressive systems tract: the Pleistocene Higashikanbe Gravel, central Japan. *Sedimentology* **47**(1): 135–149.
How P, Schild KM, Benn DI *et al*. 2019. Calving controlled by melt-under-cutting: detailed calving styles revealed through time-lapse observations. *Annals of Glaciology* **60**(78): 20–31.
How P, Messerli A, Mätzler E *et al*. 2021. Greenland-wide inventory of ice marginal lakes using a multi-method approach. *Scientific Reports* **11**: 4481.
Hubbard A, Bradwell T, Golledge N *et al*. 2009. Dynamic cycles, ice streams and their impact on the extent, chronology and deglaciation of the British-Irish ice sheet. *Quaternary Science Reviews* **28**: 758–776.
Iverson NR, McCracken RG, Zoet LK *et al*. 2017. A theoretical model of drumlin formation based on observations at Múlajökull, Iceland. *Journal of Geophysical Research: Earth Surface* **122**: 2302–2323.
Jamieson SSR, Stokes CR, Livingstone SJ *et al*. 2016. Subglacial processes on an Antarctic ice stream bed. 2: Can modelled ice dynamics explain the morphology of mega-scale glacial lineations? *Journal of Glaciology* **62**(232): 285–298.
Kellerer-Pirklbauer A, Avian M, Benn DI *et al*. 2021. Buoyant calving and ice-contact lake evolution at Pasterze Glacier (Austria) in the period 1998-2019. *The Cryosphere* **15**: 1237–1258.
King EC, Hindmarsh RCA, Stokes CR. 2009. Formation of mega-scale glacial lineations observed beneath a West Antarctic ice stream. *Nature Geoscience* **2**(8): 585–588.
Kirkbride MP, Warren CR. 1997. Calving processes at a grounded ice cliff. *Annals of Glaciology* **24**: 116–121.
Kokalj Ž, Zakšek K, Oštir K. 2011. Application of sky-view factor for the visualization of historic landscape features in LiDAR-derived relief models. *Antiquity* **85**(327): 263–273.
Lang J, Sievers J, Loewer M *et al*. 2017. 3D architecture of cyclic-step and antidune deposits in glacigenic subaqueous fan and delta settings: integrating outcrop and ground-penetrating radar data. *Sedimentary Geology* **362**: 83–100.
Long M. 2019. The second Hanrahan Lecture: geotechnical properties of Irish compressible soils. *Quarterly Journal of Engineering Geology and Hydrogeology* **53**(4): 475–523.
Long M, O'Riordan NJ. 2001. Field behaviour of very soft clays at the Athlone embankments. *Géotechnique* **51**: 293–309.
Lønne I, Nemec W. 2011. Modes of sediment delivery to the grounding line of a fast-flowing tidewater glacier: implications for ice-margin conditions and glacier dynamics. *Geological Society of London Special Publication* **354**: 33–56.
Lowe DR. 1979. Sediment gravity flows: their classification and some problems of application to natural flows and deposits. *SEPM Special Publications* **27**: 75–82.
Lowe DR. 1982. Sediment gravity flows II: depositional models with special reference to the deposits of high-density turbidity currents. *Journal of Sedimentary Petrology* **52**: 279–297.
Maizels J. 1989. Sedimentology, paleoflow dynamics and flood history of jökulhlaup deposits: paleohydrology of Holocene sediment sequences in southern Iceland sandur deposits. *Journal of Sedimentary Petrology* **59**: 204–223.
Mäkinen J, Räsänen M. 2003. Early Holocene regressive spit-platform and nearshore sedimentation on a glaciofluvial complex during the Yoldia Sea and the Ancylus Lake Phases of the Baltic Basin, SW Finland. *Sedimentary Geology* **158**(1–2): 25–56.
Marren P. 2005. Magnitude and frequency in proglacial rivers: a geomorphological and sedimentological perspective. *Earth-Science Reviews* **70**: 203–251.
Massari F. 1996. Upper-flow-regime stratification types on steep-face, coarse-grained, Gilbert-type progradational wedges (Pleistocene, southern Italy). *Journal of Sedimentary Research* **66**: 364–375.
Massari F. 2017. Supercritical-flow structures (backset-bedded sets and sediment waves) on high-gradient clinoform systems influenced by shallow-marine hydrodynamics. *Sedimentary Geology* **360**: 73–95.
Massari F, Parea GC. 1988. Progradational gravel beach sequences in a moderate- to high-energy microtidal marine environment. *Sedimentology* **35**: 881–913.
Massari F, Parea GC. 1990. Wave-dominated Gilbert-type gravel deltas in the hinterland of the Gulf of Taranto (Pleistocene, southern Italy). *Special Publication of the International Association of Sedimentologists* **10**: 311–331.
McCabe AM. 2007. *Glacial Geology and Geomorphology–The Landscapes of Ireland*. Dunedin Academic Press: Edinburgh.
McCarron S. 2013. Deglaciation of the Dungiven Basin, North-west Ireland. *Irish Journal of Earth Sciences* **31**: 43–71.
Meehan RT. 1999. Directions of ice flow during the last glaciation in counties Meath, Westmeath and Cavan, Ireland. *Irish Geography* **32**: 26–51.
Meehan RT. 2004. Evidence for several ice marginal positions in east central Ireland, and their relationship to the Drumlin Readvance Theory. In *Quaternary Glaciations-extent and chronology. Part 1: Europe*, Ehlers J, Gibbard PL (eds). Elsevier: Amsterdam; 193–194.
Mitchell GF. 1990. *Shell guide to reading the Irish landscape*. Country House: Dublin.
Mulder T, Alexander J. 2001. The physical character of subaqueous sedimentary density flows and their deposits. *Sedimentology* **48**: 269–299.
Murton DK, Murton JB. 2012. Middle and Late Pleistocene glacial lakes of lowland Britain and the southern North Sea Basin. *Quaternary International* **260**: 115–142.
Neal A, Pontee NI, Pye K *et al*. 2002. Internal structure of mixed-sand-and-gravel beach deposits revealed using ground-penetrating radar. *Sedimentology* **49**: 789–804.
Nemec W. 1990. Deltas–remarks on terminology and classification. In *Coarse-grained Deltas. Special Publication of the International Association of Sedimentologists*. Colella A, Prior D (eds). **10**: 3–12.
Nemec W, Steel RJ. 1984. Alluvial and coastal conglomerates: their significant features and some comments on gravelly mass-flow deposits. In *Sedimentology of Gravels and conglomerates*, Koster EH, Steel RJ (eds). **10** Canadian Society of Petroleum Geologists: Memoir; 1–31.
Nemec W, Lønne I, Blikra LH. 1999. The Kregnes moraine in Gudalen, west-central Norway: anatomy of a Younger Dryas proglacial delta in a paleofjord basin. *Boreas* **28**: 454–476.
Normandeau A, Dietrich P, Clarke JH *et al*. 2019. Retreat pattern of glaciers controls the occurrence of turbidity currents on high-latitude fjord deltas (Eastern Baffin Island). *Journal of Geophysical Research, Earth Surface* **124**(96): 1559–1571.
Ojala AEK. 2016. Appearance of De Geer moraines in southern and western Finland–implications for reconstructing glacier retreat dynamics. *Geomorphology* **255**: 16–25.
Pascucci V, Martini IP, Endres AL. 2009. Facies and ground-penetrating radar characteristics of coarse-grained beach deposits of the uppermost Pleistocene glacial lake Algonquin, Ontario, Canada. *Sedimentology* **56**: 529–545.
Pellicer XM, Warren WP. 2005. *Eskers and associated landforms and deposits: the key to the pattern of deglaciation in the midlands of Ireland*. Abstract, International Association of Geomorphologists, 6th International Conference on Geomorphology, 7–11 September, 2005, Zaragoza, Spain.
Pellicer XM, Warren WP, Gibson P *et al*. 2012. Construction of an evolutionary deglaciation model for the Irish midlands based on the integration of morphostratigraphic and geophysical data analyses. *Journal of Quaternary Science* **27**(8): 807–81.
Philcox ME. 2019. *Glacial Lake Blessington: deposits, deformation, outflow features*. INQUA 2019 Field Guide M:GL-3. Irish Quaternary Association: Dublin.
Pierson TC. 1981. Dominant particle support mechanism in debris flows at Mt. Thomas, New Zealand and implications for flow mobility. *Sedimentology* **28**: 49–60.
Pierson TC. 1985. Initiation and flow behaviour of the 1980 Pine Creek and Muddy River lahars, Mount St. Helens, Washington. *Geological Society of America Bulletin* **96**: 1056–1069.

Ponce JF, Guilllot MG, Balocchi LD *et al*. 2019. Geomorphological evidences of paleosurge activity in Lake Viedma Lobe, Patagonia, Argentina. *Geomorphology* **327**: 511–522.

Postma G. 1983. Water escape structures in the context of a depositional model of a mass flow dominated conglomeratic fan-delta. *Sedimentology* **30**: 91–103.

Postma G. 1990. Depositional architecture and facies of river and fan deltas: a synthesis. In *Coarse-grained DeltasSpecial Publication of the International Association of Sedimentologists*. Colella A, Prior D (eds). **10**: 13–28.

Postma G, Roep TB. 1985. Resedimented conglomerates in the bottomsets of Gilbert-type gravel deltas. *Journal of Sedimentary Petrology* **55**(6): 874–885.

Roberts DH, Ó Cofaigh C, Ballantyne CK *et al*. 2020. The deglaciation of the western sector of the Irish Ice Sheet from the inner continental shelf to its terrestrial margin. *Boreas* **49**(3): 438–460.

Russell AJ, Roberts MJ, Fay H *et al*. 2006. Icelandic jökulhlaup impacts: Implications for ice-sheet hydrology, sediment transfer and geomorphology. *Geomorphology* **75**: 33–64.

Rust BR. 1977. Mass flow deposits in a Quaternary succession near Ottawa, Canada: diagnostic criteria for subaqueous outwash. *Canadian Journal of Earth Sciences* **14**: 175–184.

Sambrook Smith GH. 2000. Small-scale cyclicity in an alpine proglacial fluvial sedimentation. *Sedimentary Geology* **132**: 217–231.

Sanders D. 2000. Rocky shore-gravelly beach transition, and storm-post-storm changes of a Holocene gravelly beach (Kos Island, Aegean Sea): stratigraphic significance. *Facies* **42**: 227.

Schild KM, Renshaw CE, Benn DI *et al*. 2018. Glacier calving rates due to subglacial discharge, fjord circulation and free convection. *Journal of Geophysical Research: Earth surface* **123**: 2189–2204.

Schomacker A. 2010. Expansion of ice-marginal lakes at the Vatnajökull ice cap, Iceland, from 1999 to 2009. *Geomorphology* **119**: 232–236.

Sevastopulo GD, Wyse-Jackson PN. 2009. Carboniferous: Mississippian (Tournaisian and Viséan). In *The Geology of Ireland*, Holland C, Sanders I (eds). 2nd ed. Dunedin Academic Press: Edinburgh; 215–268.

Shennan I, Bradley SL, Edwards R. 2018. Relative sea-level changes and crustal movements in Britain and Ireland since the Last Glacial Maximum. *Quaternary Science Reviews* **188**: 143–159.

Shugar D, Burr A, Haritashya UK *et al*. 2020. Rapid worldwide growth of glacial lakes since 1990. *Nature Climate Change* **10**: 939–945.

Slater DA, Benn DI, Cowton TR *et al*. 2021. Calving multiplier effect controlled by melt undercut geometry. *Journal of Geophysical Research Earth Surface* **126**: e2021JF006191.

Smith AM, Murray T. 2009. Bedform topography and basal conditions beneath a fast-flowing West Antarctic ice stream. *Quaternary Science Reviews* **28**(708): 584–596.

Smith GA. 1986. Coarse-grained nonmarine volcaniclastic sediment: terminology and depositional process. *Geological Society of America Bulletin* **97**: 1–10.

Smith ND. 1974. Sedimentology and bar formation in the upper Kicking Horse River, a braided outwash stream. *Journal of Geology* **81**: 205–223.

Smith ND. 1990. The effects of glacial surging on sedimentation in a modern ice-contact lake, Alaska. *Geological Society of America Bulletin* **102**: 1393–1403.

Sollas WJ. 1896. A map to show the distribution of eskers in Ireland. *Royal Dublin Society Scientific Transactions 5(Series 2)* 785–822.

Stokes CR, Clark CD. 2003. The Dubawnt Lake palaeo-ice stream: evidence for dynamic ice sheet behaviour on the Canadian Shield and insights regarding the controls on ice stream location and vigour. *Boreas* **32**: 263–279.

Storrar R, Jones AH, Evans DJA. 2017. Small-scale topographically-controlled glacier flow switching in an expanding proglacial lake at Breidamerkurjökull, SE Iceland. *Journal of Glaciology* **63**(240): 745–750.

Sugiyama S, Minowa M, Sakakibara D *et al*. 2016. Thermal structure of proglacial lakes in Patagonia. *Journal of Geophysical Research, Earth Surfaces* **121**: 2270–2286.

Sutherland JL, Carrivick JL, Gandy N *et al*. 2020. Proglacial lakes control glacier geometry and behaviour during recession. *Geophysical Research Letters* **47**(19): e2020GL088865.

Synge FM. 1952. Retreat stages of the last ice-sheet in the British Isles. *Irish Geography* **2**(4): 168–171.

Synge, FM. 1979. *Quaternary glaciation in Ireland. Quaternary Newsletter* **28**: 1–18

Synge FM, Mitchell GF, Warren WP *et al*. 1975. Field guide to the Quaternary of the Wicklow District. *Quaternary Research Association Field Guide*

Teller JT. 2005. Subaquatic Landsystems: Large Proglacial Lakes. In *Glacial Landsystems*. Evans DJA (ed). Hodder Arnold; 348–371.

Teller JT, Leverington DW. 2004. Glacial Lake Agassiz: a 5000 yr history of change and its relationship to the $\delta^{18}O$ record of Greenland. G*eological Society of America Bulletin* **16**(5–6): 729–742.

Tomura T. 2012. Beach ridges and prograded beach deposits as palaeoenviroment records. *Earth-Science Reviews* **114**: 279–297.

Tsutaki S, Fujita K, Nuimura T *et al*. 2019. Contrasting thinning patterns between lake- and land-terminating glaciers in the Bhutanese Himalaya. *The Cryosphere* **13**: 2733–2750.

Utting DJ, Atkinson N. 2019. Proglacial lakes and the retreat pattern of the southwest Laurentide Ice sheet across Alberta, Canada. *Quaternary Science Reviews* **225**: 106034.

Van der Meer JJM, Warren WP. 1997. Sedimentology of late glacial clays in lacustrine basins, Central Ireland. *Quaternary Science Reviews* **16**: 779–791.

Warren CR, Kirkbride MP. 2003. Calving speed and climatic sensitivity of New Zealand lake-calving glaciers. *Annals of Glaciology* **36**: 173–178.

Warren CR. 1994. Freshwater calving and anomalous glacier oscillations: recent behaviour of Moreno and Ameghino Glaciers, Patagonia. *Holocene* **4**(4): 422–429.

Warren WP. 1991. *Ireland. Field Guide for INQUA excursion*. Unpublished.

Warren WP, Ashley GM. 1994. Origins of the ice-contact stratified ridges (Eskers) of Ireland. *Journal of Sedimentary Research* **A64**: 433–449.

Winsemann J, Hornung JJ, Meinsen J *et al*. 2009. Anatomy of a subaqueous ice-contact fan and delta complex, Middle Pleistocene, North-west Germany. *Sedimentology* **36**: 1041–1076.

Winsemann J, Brandes C, Polom U. 2011. Response of a proglacial delta to rapid high-amplitude lake level change: an integration of outcrop data and high resolution shear wave seismic. *Basin Research* **23**: 22–52.

Winsemann J, Lang J, Polom U *et al*. 2018. Ice-marginal forced regressive deltas in glacial lake basins: geomorphology, facies variability and large-scale depositional architecture. *Boreas* **47**: 973–1002.

Zakšek K, Oštir K, Kokalj Ž. 2011. Sky-view factor as a relief visualization technique. *Remote Sensing* **3**: 398–415.

